國立臺灣大學醫學院微生物學科暨研究所

碩士論文

Graduate Institute of Microbiology
College of Medicine
National Taiwan University

Master Thesis

NRIP 缺陷小鼠造成心室肥大

Deficiency of NRIP causes cardiac hypertrophy

林思瑜

Ssu-Yu Lin

指導教授：陳小梨 博士

Advisor: Show-Li Chen, Ph.D.

中華民國 101 年 7 月

July, 2012

國立臺灣大學（碩）博士學位論文
口試委員會審定書

中文題目：NRIP缺陷小鼠造成心室肥大

英文題目：Deficiency of NRIP causes cardiac hypertrophy

本論文係林思瑜君（學號R94445121）在國立臺灣大學微生物學所完成之碩（博）士學位論文，於民國101年7月26日承下列考試委員審查通過及口試及格，特此證明

口試委員：

陳小梨（簽名）

（指導教授）

陳佑宗	顏茂庭
薛殷泰	

系主任、所長 鄧述諄（簽名）

致謝

經過兩年多來的努力，我終於要畢業了!耶!開心!首先，我要感謝實驗室的大家長，小梨老師。謝謝老師給我機會進到溫馨的R710裡學習，也謝謝老師讓我見識到科學人的模樣。每當實驗遇到瓶頸時，老師總用她對科學研究的熱誠跟勇於嘗試的精神，鼓勵我們挑戰新的事物，追求突破。也因為老師的勇於冒險，才能有今天這篇論文的產生，謝謝老師。

回顧兩年多來的生活,幾乎與R710的夥伴們日夜相伴。領我入門的思為學長，雖然常常覺得你對實驗的那份嚴謹的態度令人吃不消，但是我也很感謝因為有你的要求，我才能更進步。常常邊念卻邊幫我收拾爛攤子的秉昌學長，實驗室能有你在真的很好,希望以後還能一起去扭蛋!同一條bench的曉慧學姊,感謝你總是有耐心的傾聽我的煩惱(抱怨?)，另外忍不住要說，生蠔真的超好吃!三人成虎的成員，大受抱怨一姊其害的楚崴學長，跟你在一起總是無限歡樂，你是真的很B型，而我不久的將來也會真正成為伯瀚學長口中的那個電梯口學妹,plz wait!給嚴謹的伯瀚學長，雖然常取笑你，但是你對事情認真負責的態度，真的是值得我好好學習的對象,而且以後蘇阿姨我們不會再遲到囉!給立博學長跟Sammin姊，感謝你們總是為實驗室帶來許多歡笑,學長不要再下二抗了!動物實驗權威信雄學長，感謝你總是幫我配動物跟拿老鼠，雖然身為學妹說這樣的話似乎很不應該!身在遠方的郁婷學姊，我很想再跟小林尊一起吃遍美食，超級懷念烏來第一湯。網拍一姊佳怡學姊，你的共筆真的令人超感動，也很懷念跟團的時光，團長快回來。趕畢業這段期間幫我分擔很多工作的未辰跟元駿，未辰希望你能在畢業前嚐遍台灣各地的好吃甜食，元駿祝你成為動物實驗的新一代強人。R710裡，要感謝的太多了，感謝你們容忍暴走一姊，現在大家的耳朵終於要解脫了!

感謝中研院的顏裕庭老師,以及他們實驗室的燕玲跟其他學長姐們。沒有你們的大力相助,這本論文恐怕沒辦法如此順利的完成。感謝陳文彬老師跟倖慧學姊，有你們大力幫助，大方借用實驗室，讓我在最後這段趕data的日子，能有多一點時間練習，才能順利趕完最後的實驗。感謝蘇銘嘉老師與陳佑宗老師，在每一次的committee裡總是提供我許多寶貴的意見，幫助我順利完成論文。

最後，我要感謝最愛的家人，媽媽無怨無悔的支持，妹妹時時的關心，爸爸跟弟弟的陪伴。因為有你們在，回家就可以洗去一切的疲憊，重新出發。最後最後，還有兩年來給予我最大包容，最多依靠的德哥，感謝你容忍我的任性，跟我一起分享快樂與悲傷，有你跟藍藍，即使實驗做到很晚回家，也不孤單。謝謝，大家跟這一切。

中文摘要

我們實驗室在2005年發現了一個基因，命名為nuclear receptor interaction protein (縮寫：NRIP，又名 DCAF6 或 IQWD1)。NRIP 的蛋白質結構由七個 WD-40 repeats 以及一個 IQ motif 所組成。且實驗室先前的研究證明在有鈣離子的情況下，NRIP 會利用 IQ motif 與調鈣素（Calmodulin）下進行交互作用。利用實驗室的 NRIP 基因剔除小鼠進行行為測試，其結果暗示 NRIP 可能參與心臟功能的調控。因此，我們利用心臟超音波檢測，針對NRIP基因剔除小鼠進行長期性的心臟功能監測。根據監測的結果，我們發現剔除 NRIP 基因確實會影響到小鼠的心臟功能，並且伴隨著年紀增長，心肌有趨於肥厚的現象（cardiac hypertrophy）。為了進一步驗證這項發現，我們將小鼠的心臟取出進行一連串的組織分析，得到的結果與心臟超音波的結果一致。在年紀大的基因剔除小鼠中，我們不但找到心肌肥厚的現象，還發現這些老鼠有心肌纖維化的情形發生。

所以，為了找出 NRIP 調節心臟功能的分子機制，我們進一步利用 yeast two-hybrid 進行大量篩選，發現到一群屬於 α-actinin 家族的蛋白質會與 NRIP 產生交互作用。α-actinin 有四種異構型，其中特定表現在肌肉細胞的異構型 ACTN2 是組成肌節上 Z-disc 的主要成分。Z-disc 可以與肌動蛋白絲連結，是維持肌節構形以及穩定肌肉收縮的重要結構。因此，我們利用 in vitro 及 in vivo binding assay 進一步確認了 NRIP 與 ACTN2 的交互作用，之後又分析兩者間交互作用的區塊並且利用免疫螢光染色法，證明兩者在組織中共同存在於 Z-disc 上，也意外發現了 NRIP 是一個新的 Z-disc protein。然而，許多論文指出 Z-disc protein 一旦有缺失便會造成肌節排列錯亂，影響心臟功能而導致心肌症（cardiomyopathy）。因此，我們利用穿透視電子顯微鏡來觀察 NRIP 基因剔除小鼠的肌節構造。結果顯示缺少 NRIP 的小鼠其肌節的結構受到影響，特別的是肌節的 I-band 變窄以及 Z-disc

變寬。另外，實驗室先前的研究證實 NRIP 會在有鈣離子的情況下與調鈣素(calmodulin)交互作用，且許多研究指出調鈣素在心肌細胞裡，可以與許多鈣離子通道或者與其他蛋白質交互作用，直接或間接的影響心肌細胞內鈣離子濃度的變化。因此，我們純化並檢測老鼠心肌細胞收縮時鈣離子的變化，發現缺少 NRIP 會影響心肌細胞收縮時的鈣離子變化量。根據目前的證據我們作出以下的推論：NRIP 是一個能夠與 ACTN2 進行交互作用的 Z-disc protein，且缺少 NRIP 會影響肌節的結構，以及心肌細胞收縮時鈣離的變化量，進而導致心臟收縮功能受損，而引發最終我們看到的心肌肥大的結果。

關鍵字：NRIP、IQ motif、ACTN2、Z-disc、cardiomyopathy。

Abstract

Previously, we demonstrated a novel gene, nuclear receptor interaction protein (NRIP, also named as DCAF6 or IQWD1), which could cooperate with nuclear receptors such as androgen and glucocorticoid receptors and its gene expression was regulated by androgen via androgen receptor. We also identified NRIP as a Ca^{2+}-dependent calmodulin binding protein that activates calcineurin phosphatase activity. To investigate insights into *in vivo* function of NRIP, we generated *NRIP*-null mice and found that loss of NRIP impairs cardiac function and lead to cardiac hypertrophy progressively. Furthermore, $NRIP^{-/-}$ mice display weaker muscle strength, reduced cardiac function, and cardiac fibrosis at elder stage compared with WT. To verify the regulatory mechanism, we found that α-actinin-2 (ACTN2), which is a biomarker of muscular Z-disc complex is one of NRIP-interacting proteins from the yeast two-hybrid system. ACTN2 cross-links with actin filament to stabilize sarcomeric structure and muscle contraction, which is an essential constituent of sarcomere. Through the *in vitro* and *in vivo* binding assays, we further confirmed the interaction and defined the interacting domains between NRIP and ACTN2. Plus co-localization of NRIP and ACTN2 was discovered in cardiac tissue by immunofluorescence assays,

we firstly defined NRIP as a Z-disc protein. Although the Z-disc has been viewed as a passive constituent of the sarcomere traditionally, increasing numbers of mutations in Z-disc proteins leading to disruption and malfunction of the contractile apparatus have been shown to cause cardiomyopathies and/or muscular dystrophies. Hence, we analyzed the sarcomeric structure of NRIP$^{-/-}$ cardiomyocytes and found reduction of I-band width and extension of Z-disc. Besides, we know that NRIP is a Ca^{2+}-dependent calmodulin binding protein. In cardiomyocytes, calmodulin interacts with multiple calcium ion channels or proteins to directly or indirectly regulate the variation of calcium concentration during muscle contraction. Therefore, we isolated and measured the calcium transient of cardiomyocytes. Then, we found that deficiency of NRIP decreases the amplitude of calcium transient. In a conclusion, we speculated that loss of NRIP impairs the structure of sarcomere, the amplitude of calcium transient during muscle contraction and the function of muscle contraction resulting in cardiomyopathy.

Key word: NRIP, IQ motif, ACTN2, Z-disc, cardiomyopathy

Table of Contents

Chapter 1

INTRODUCTION

1.1 The background knowledge of nuclear receptor interaction protein, NRIP.

We previously identified a novel gene, nuclear receptor interaction protein (NRIP) (GenBank accession numbers AY766164 and AAX09330). NRIP has been proved as a transcriptional co-activator, which up regulates androgen receptor (AR) and glucocorticoid receptor (GR)-driven transcriptional activity in a ligand-dependent manner. (Tsai et al, 2005) Reciprocally, the gene expression of NRIP is regulated by androgen via androgen receptor (Chen et al, 2008). The protein of NRIP is composed of 860 amino acids containing with seven WD-40 repeats and one IQ motif (Chang et al, 2011; Tsai et al, 2005). The IQ motif has been reported as an interaction domain of EF-hand motif containing protein, such as calmodulin (Bahler & Rhoads, 2002). Therefore, we have proved the interaction of NIRP and calmodulin in a calcium-dependent manner (Chang et al, 2011).

In the study of Tsai et al, the mRNA of NRIP is over-expressed in skeletal muscles, hearts, and testis. Previously, we found that NRIP$^{-/-}$ mice showed worse motor performance in rotarod and treadmill tests (Chen HH, unpublished data) and weaker contraction force in the muscle contractility measurement by using diaphragms and

soleus (Chen HH, unpublished data). Also, the study of limb-girdle muscular dystrophy (LGMD) indicates gene expression of IQWD1 (another name of NRIP) is low in AR-LGMD patients (Zhang et al, 2006). These results are consistent with our speculation and imply that NRIP might not only play roles in prostates, but also in striated muscles.

1.2 Abnormality of calcium homeostasis or sarcomeric proteins leads to cardiomyopathy.

Cardiomyopathy is a disorder of cardiac muscles; cardio- refers as "heart" and myo- refers as "muscle". It leads to myocardial hypertrophy and in long-term predisposes individuals to heart failure, arrhythmia and sudden death resulting in a life-threatening illness (Frey & Olson, 2003; Heineke & Molkentin, 2006). Biochemical or mechanical stimuli can induce a phase of cardiac hypertrophy, which might be compensated hypertrophy, the phenotypes include that myocytes grow in length and/or width as means of increasing cardiac pump function and decreasing ventricular wall tension (Frey & Olson, 2003; Heineke & Molkentin, 2006). Based on the predominant pathophysiological feature, cardiomyopathies are classified into ischemia or non-ischemia cardiomyopathies. Non-ischemia cardiomyopathies are further grouped into dilated, hypertrophic and restrictive cardiomyopathies

(Richardson et al, 1996). According to recent studies, mutations or deletions of sarcomeric and cytoskeletal proteins predispose to non-ischemia cardiomyopathy, such as cardiac hypertrophy or dilated cardiomyopathy (Arber et al, 1997; Chien, 1999; Hemler, 1999). Therefore, investigations of these proteins help to clarify the causes of cardiomyopathies.

Except the defect of sarcomeric structure, the abnormality of calcium homeostasis also leads to cardiomyopathies. Calcium homeostasis in cardiac myocytes is important for the function of contraction (Barry & Bridge, 1993). Excitation-contraction (EC) coupling is a physiological process of converting an electrical stimulus to a mechanical response (Sandow, 1952), which involves calcium activation of contractile proteins and the removal of calcium facilitating relaxation. Recent studies indicates that EC-coupling plays a critical role in the pathophysiology of myocardial failure (Hasenfuss, 1998). The altered expression of the genes involving in calcium handling, such as Ca^{2+}-ATPase (SERCA2), ryanodine receptor (RYR2) and phospholamban (PLN), results in failing hearts (Arai et al, 1993; Hasenfuss, 1998; Pieske et al, 1999).

1.3 Z-disc protein, sarcomere structure and cardiomyopathy.

Z-disc is the sarcomeric structure forming the boundary of sarcomere in striated muscles by cross-linking with actin filament, nebulin/nebulette and titin to stabilize the

muscle contraction and to transmit the force generated by the myofilaments. Numerous Z-disc proteins have been investigated and functioned as a structural support (Arber et al, 1997; Hassel et al, 2009; Witt et al, 2006). According to these studies, mutations or deletions of Z-disc proteins disrupt sarcomere arrangement, affect cardiac function and ultimately lead to cardiomyopathy (Knoll et al, 2011) including MLP (Arber et al, 1997), nexilin (Hassel et al, 2009), cypher and calsarcin1 and α-actinin. In addition to a structural support, recent studies indicate that Z-disc is also a nodal point to transduce biochemical or mechanical signals to other cellular compartment such as nucleus (Frank et al, 2006).

1.4 The characteristic of ACTN2.

α-Actinin (ACTN) belongs to a spectrin superfamily, which consist of actin-bundling and membrane-anchoring proteins, like α-actinin, dystrophin/utrophin and spectrin. Proteins of spectrin family are arisen from a common ancestral *α*-actinin gene and characterized by the presence of spectrin repeats, actin-binding domains, and EF-hands (Broderick & Winder, 2005). α-Actinin has four isoforms including ACTN1 to 4. Non-muscle isoforms, ACTN1 and ACTN4, are associated with focal contacts and stress fibers; muscle isoforms, ACTN2 and ACTN3, are localized in Z-disc and stabilize the muscle contractile apparatus. Among these two isoforms, ACTN2 is a

major constituent expressed in the cardiac and oxidative skeletal muscle while ACTN3 is largely expressed in glycolytic skeletal muscle fibers (Sjoblom et al, 2008). In cardiac muscles, ACTN2 cross-links with actin filaments and associates with cytoskeletal proteins. Therefore, it is not only an important structural protein but also the regulator of cytoskeleton organization and muscle contraction. Recent studies indicate that ACTN2 also associates with a number of signaling molecules, such as cytoplasmic domains of transmembrane receptors and ion channels (Cukovic et al, 2001; Sadeghi et al, 2002). Because of the structural and signaling importance of ACTN2, mutations in ACTN2 lead to cardiomyopathies. From patients affected by cardiomyopathy, some studies find mutations in ACTN2 gene. A single mutation Gln9Arg of ACTN2 has been reported from an individual affected by dilated cardiomyopathy (DCM) (Mohapatra et al, 2003). And from patients with hypertrophic cardiomyopathy (HCM), more mutations, Ala119Thr, Thr495Met, Glu583Ala, and Glu628Gly of ACTN2 have been identified (Chiu et al, 2010).

1.5 Aims of this study

According to the description above, we know that NRIP is highly expressed in striated muscles and deficiency of NRIP impairs muscle contractility. Therefore, we speculate that NRIP might paly a role in regulating cardiac function. Hence, the following are our aims of this study:

(a) To verify whether loss of NRIP lead to cardiac function defects and cardiomyopathy.

(b) To reveal the cause of NRIP affecting cardiac function in a molecular manner, finding out the interacting protein of NRIP.

(c) To define the interacting domain between NRIP and the interacting protein, ACTN2.

(d) To confirm whether lack of NRIP leads to sarcomeric structural effects.

(e) To investigate whether loss of NRIP affects the calcium transient of cardiomyocytes.

Chapter 2

MATRRIALS AND METHODS

2.1 Plasmids and constructs

GST-ACTN1, ACTN2 and ACTN2-V5 were cloned in frame into pGEX-4T-1 (GE) and pcDNA3.1-V5-His vectors, by PCR amplification using specific primers containing restriction sites. The cDNA used to amplification were extracted from SJ-RH30 cell (Human rhabdomyosarcoma cell line). GST-ACTN2ΔEF-hand was cloned in frame into pGEX-4T-1 vector, by using GST-ACTN2 as a template to amplify the sequence of ACTN2 (1-750 amino acids). His-MBP- NRIP and EGFP-NRIP were cloned in frame into pMAL-c2X (NEB) and pEGFP-C1 (Clontech) from predecessors. The following forward and reverse primers were used:

GST-ACTN2-F: 5'-AAAA GAATTC ATGAACCAGATAGAGCCCGGC-3';

GST-ACTN2-R: 5'-AAAA CTCGAG TCACAGATCGCTCTCCCCGTA-3'

GST-ACTN2-1-750-R: 5'-AAAA CTCGAG TCA GATGCCCTTCGCATCTC

TCG-3';ACTN2-V5-F: 5'-AAAA GAATTC ATGAACCAGATAGAGCCCGGC-3';

ACTN2-V5 R: 5'-CAGATCGCTCTCCCCGTAGAG-3';

2.2 Cell culture

293T cells derived were maintained in DMEM (Dulbecco's modified Eagle's medium) with 10% FBS (fetal bovine serum), 100U/ml of penicillin G and 100U/ml of streptomucin, 2mM l-glutamine at 37°C and 5% CO_2. SJ-RH30 cell were maintained in RPMI 1640 medium supplemented with 10% FBS, 2 mM L-glutamine and antibiotics at 37°C and 5% CO_2.

2.3 *In vitro* Binding Assay

Recombinant GST-ACTN2 and GST-ACTN2ΔEF-hand were expressed in bacteria (*Rosetta*) at 16°C. Further purification was performed using glutathione sepharose beads (GE). His-MBP-NRIP and its truncated mutants were also expressed in bacteria (*Rosetta*) at 16°C and purified by using amylose resin (New England Bio Labs). In detail, add the plamids (2 μl, 1μg/μl) described above into 20 μl *E. coli* (*Rosetta*) and incubate on ice for 3min then heat shock at 42°C for 90 sec. Put it on ice for 3min then add 500μl LB broth and seed 50μl into Amp-containing plate (Kana-containing palte were used for His-MBP-NRIP and its truncated mutants) for overnight (16hr) at 37°C incubation. The next day, pick one colony for small preparation at 37°C 16 hr incubation in 3ml LB containing ampicillin. Then pour 400μl bacteria culture into 200ml LB containing ampicillin for 3hr shaking at 37°C till the optical density reaches

0.6. Expression of the recombinant proteins was induced by the addition of 1mM IPTG (isopropyl-beta-D-thiogalactopyranside) at 16°C overnight. Bacteria lysates were harvested by centrifugation at 8000rpm 4°C for 10min. Then the pellets were resuspended by sonication buffer (50 mM NaH_2PO_4, 300 mM NaCl, 20% glycerol pH8.0 add DTT,PMSF to 1mM before use) and put on ice for 10min. Sonication on ice with energy level 4, 10 sec pulse with 15 sec interval, total 60 repeats. Spin at 10000rpm for 10min at 4°C and freeze the supernatant that containing recombinant proteins in -20°C. The GST-tagged proteins are purified by incubation with glutathione-sepharose 30μl beads for 1.5 hr at 4°C. Wash the GST-fusion protein conjugated beads by sonication buffer three times. Add 1ml co-IP buffer (20mM Tris, 150mM NaCL, 10% glycerol, 0.1% NP-40, 5mM $MgCl_2$ pH 7.5, 1mM EDTA and 1mM DTT protease inhibitor were added before use). His-tagged proteins were incubated with GST protein-conjugated beads for 1.5hr at 4°C. Then spin down the beads and washed by co-IP buffer three times. Samples can be eluted by 2x sample buffer for subsequent Western blot analysis. Antibodies are used in Western blot detection: NRIP 1:1000 (Gene Tex), α-actinin 1: 5000 (abcam).

2.4 Transfection and Immunoprecipitation assay

Prior to transfection, cells were seeded in 6-cm dish at a density of 2×10^6 per well

in DMEM with 5% dextran-coated charcoal- stripped FBS (DCCS-FBS) (HyClone) for 24 h. Transient transfections of cells were performed using calcium phosphate with various reporter plasmids, 10μg of EGFP-NRIP, 2μg of ACTN2-V5 and 2μg of pEGFP-C1 and pcDNA3.1-V5-His as internal control. EGFP-NRIP and ACTN2-V5 plasmids were transfected into 293T cells for 48hr, then the protein lysates were collected by 0.1% NP-40 buffer with sonication (150mM NaCl, 50mM Tris-HCl, 0.1% NP-40 pH 8.0). Mixed 500μg protein lysates with 0.1% NP-40 buffer to total 700μl, and add 1mg anti-EGFP or anti-V5 antibodies then incubated at 4°C overnight. The next day, add 40μl agarose beads into the lysates then incubated at 4°C for 1.5hr. After that, spin down the beads and washed with 0.1% NP-40 twice. Then eluted proteins by 2x sample buffer for subsequent Western blot analysis. Antibodies are used in Western blot detection: anti-V5 1:3000 (Invitrogen), anti-GFP 1:3000 (Clonetech).

2.5 Western blot analysis

For western blot, samples prepared form previous experiments were loaded into 10% SDS-PAGE, set constant voltage at 80V for stacking, and run at 140V for separating.

2.6 Histological analysis

Hearts were excised form WT or NRIP$^{-/-}$ mice, and perfused with 0.5% lidocaine and fixed with 4% paraformaldehyde (PFA) at 4°C overnight. Hearts for histological analysis all followed with this procedure except the immunofluorence assay (IF). Hearts were used for IF without fixing with PFA.

2.7 Hematoxylin and Eosin (H&E) Staining Protocol

First, put sections at 70°C for 30min to melt the paraffin. Then put sections into xylene (two sets of xylene were prepared) for 10min each to deparaffinize sections. After that re-hydrate sections with absolute alcohol for 10min. Then put sections progressively into 100%, 90%, 80%, 70% and distilled water for 5min each. Stained with hematixylin solution for 2min, then wash in running tap water for 3 min. Next, stained with eosin for 30 sec, then immediately wash with absolute alcohol for six times. Finally, put sections into Xylene for unless 10min and fixed sections with mounting gel.

2.8 Immunofluorescence assay

Hearts were excised and fixed with O.C.T. at -80°C. The frozen sections were washed with 1x PBS for twice, 5 min each, and then incubated with 0.5% Triton-X 100/ 1 x PBS for 1hr. After that, washed the sections with 1x PBS for twice, 5 min

each. Then incubated with 5%BSA/1x PBS for 1hr. After that, washed with 1x PBS twice and incubated with first antibodies for 4°C overnight. The next day, washed the sections with 1 x PBS twice and incubated with second antibodies for 1hr, RT. Then stained with DAPI and fixed the sectons. First antibodies : NRIP 1:100 (Novous), ACTN2 1:100 (Sigma), Myomesin 1:200 (Hybridoma bank) Second antibodies : goat-anti-mouse-Cy3, goat-anti-rabbit-Alexa-488 1:500-1:1000 (Jackson ImmunoResearch Laboratories), Rhodamine-conjugated Phalloidin 1:200-1:500 (Sigma).

2.9 Transmission electron microscopy analysis

Hearts were excised following the description of histological analysis. Sections were prepared by the Core Facilities of Institute of Cellular, Oragnismic Biology of Academia Sinica. Sections were analyzed by transmission electron microscope (TEM). Type: Hitachi H-7000.

2.10 Antibody

Anti-NRIP (Novous), anti-ACTN2 (Sigma), anti-myomesin (Hybridoma bank), anti-V5 (invitrogen), anti-GFP (clonetech), Rhodamine-cojugated phalloidin (Sigma).

2.11 Adult cardiomyocytes isolation

First, inject mice with 0.1 ml heparin (2000IU/ml) and wait for 10 min. Then, inject mice with 0.2 ml urethane for anesthesia. After mice is fully anesthertized, open the chest and take heart out. Cannulate the heart and tie the aorta to the cannula with 5-0 silk thread. After that, perfuse the heart with Ca^{2+} free Tyrode buffer for 3 min at the rate 3ml/min. Then, switch to enzyme buffer (enzymes dissolve into perfusion buffer) and continue perfusion for 7 min at the same rate. Once the enzyme digestion is complete, trim the heart (keep the ventricles) and put the heart into Solution A buffer. Then, separate and pipette the heart into pieces gently. Next, filter the cell suspension with 250 μm filter by gravity for 15 min. Transfer the cells to 0.06 mM, 0.24 mM, 0.6 mM, 1,2mM Ca^{2+} transfer buffer step by step every 10 min. For Ca^{2+} transient measurement, transfer the cells into 1.2 mM Ca^{2+} contractility perfusion buffer. Load the fluorescent calcium indicator, Fura-2 AM (5 mM/ml), after 30 min wash the cells with 1.2 mM Ca^{2+} contractility perfusion buffer and wait for next 30 min. After that, measure the calcium transient with the cells. To measure the calcium transient, probenecid(100 μm) and glucose (10 mM) are freshly add into 1.2 mM Ca^{2+} contractility perfusion buffer for perfusion.

The following are buffers used in the experiment:

Ca^{2+} free Tyrode buffer (pH 7.4)

NaCl	135 mM
KCl	4 mM
$MgCl_2$	1 mM
HEPES	10 mM
NaH_2PO_4	0.33 mM

Perfusion buffer (Ph 7.4)

Ca^{2+} free Tyrode buffer	
Glucose	100 mM
BDM	10 mM
Taurine	5 mM

Solution A (pH 7.4)

Perfusion buffer	
BSA	5 mg/ml

Solution B (pH 7.4)

1.2 mM Ca^{2+} contractility perfusion buffer	
Glucose	5.5 mM

1.2 mM Ca^{2+} contractility perfusion buffer (pH 7.4-7.55)

NaCl	137 mM
KCl	5.4 mM
$CaCl_2$	1.2 mM
HEPES	10 mM
$MgCl_2$	0.5 mM

Transfer buffer (pH 7.4)

	Solution A	Solution B
0.06 mM Ca^{2+}	9.5 ml	0.5 ml
0.24 mM Ca^{2+}	8 ml	2 ml
0.6 mM Ca^{2+}	5 ml	5 ml
1.2 mM Ca^{2+}	0 ml	10 ml

Chapter 3

RESULTS

3.1 Loss of NRIP leads to cardiac hypertrophy progressively.

To investigate insights into the *in vivo* function of NRIP, we have generated conventional NRIP$^{-/-}$ mice as a genetic model. NRIP-null mice were observed no morphological abnormalities and appeared normal by the criteria including behavior, weight, and fertility. Intriguingly, *NRIP* mutant mice displayed significantly reduced exercise capacity according to our preliminary results of rotarod and treadmill tests (Chen HH, unpublished data). Compared with WT mice, NRIP$^{-/-}$ mice showed considerably worse motor performance in rotarod and treadmill tests indicating that NRIP deficiency might lead to muscular weakness. Moreover, NRIP was found to be over-expressed in skeletal muscle and heart (Tsai et al, 2005) based on our previous study and these observations imply that NRIP might play functional roles in striated muscle such as skeletal and cardiac tissues. To assess the difference of muscle contractibility, the diaphragms excised from WT and KO mice were subjected to measure the muscle force *in vitro*. Indeed, *NRIP* deficient diaphragm showed weaker muscle strength than WT (Chen HH, unpublished data). Regarding that myocardium also belongs to striated muscle and the result of treadmill test indicates deficient

cardiopulmonary function (Bruce, 1974),we hypothesize that NRIP might also play a role in cardiac function. To elucidate our theory, we examined the cardiac function of WT and NRIP$^{-/-}$ mice by echocardiography (Table 1) from young to middle aged stage. According to the results, the measurements of ejection fraction (EF) and fraction shortening (FS) from NRIP$^{-/-}$ mice are lower than WT implying that NRIP$^{-/-}$ mice have cardiac functional defects. Additionally, the dimension of left ventricle, interventricular septum (IVSd), posterior wall (PW) and left ventricle mass were increased with aging showing that NRIP$^{-/-}$ mice were on the process of cardiac hypertrophy to dilated cardiomyopathy. By comparing the hearts excised at 12 and that at 39 weeks, the sizes of ventricle and atrium were enlarged at elder stages (Figure 1). As shown in Figure 2A, the histological analysis using hematoxylin and eosin (H&E) staining indicates that left ventricle walls, such as IVS and PW, were thicken in the 12-week-old NRIP$^{-/-}$ mice, but the chamber size in NRIP$^{-/-}$ mice was similar with WT. Comparing with the data shown in Figure 3A, except the thickened IVS and PW, we also found the chambers of left and right ventricles were dilated in the 39-week-old NRIP$^{-/-}$ mice which are consistent with conclusions of echocardiography. Besides, the sizes of cardiomyocytes were increased at 12 and 39-week-old NRIP$^{-/-}$ mice comparing with that in WT (Figure 2B and 3B). Statistical analyses of cell sizes and number in WT and NRIP$^{-/-}$ further elucidate the hypertrophy of NRIP$^{-/-}$ cardiomyocytes (Figure 2C-D and Figure 3C-D)..

Accompanied with dilated cardiomyopathy, histological analysis with Massion's trichrome staining revealed significantly fibrosis in the hearts of NRIP$^{-/-}$ mice compared to WT mice at 39 weeks (Figure 4). Taken together, *NRIP* deficiency in mice leads to progressively dilated cardiomyopathy and fibrosis in an age-dependent manner.

3.2 NRIP interacts with a Z-disc protein, α-actinin-2, which is a major component of cardiac Z-disc apparatus maintaining the sarcomeric structure.

To investigate the molecular insights of cardiac hypertrophy in NRIP$^{-/-}$ mice, a yeast two-hybrid screen was performed the full-length of NRIP as bait. Based on the results of two-hybrid protein-protein interaction assay, we speculated that the interactive proteins of NRIP in a great majority belonged to the α-actinin family including α-actinin 1 to 4, each found within a specific tissue type and expression profile and these proteins can be grouped into two distinct classes: muscle (2 and 3) and non-muscle cytoskeletal (1 and 4) isoforms (Sjoblom et al, 2008). Both muscle isoforms (2 and 3) are commonly expressed in skeletal, cardiac, and smmoth muscle tissue and α-actinin-2 (ACTN2) is a major component of Z-disc in cardiac muscle (Sjoblom et al, 2008). Thus, we conjectured that NRIP might affect cardiac function through interacting with ACTN2. To confirm our suggestion plus the result of yeast

two-hybrid assay, we performed *in vitro* and *in vivo* protein-protein interaction assays. Both recombinant GST-tagged ACTN1 or ACTN2 and His-tagged NRIP proteins expressed in bacteria were subjected to perform the *in vitro* binding assay (Figure 5). As shown in Figure 5C (lane 6), NRIP was found to interact with ACTN2 *in vitro*, and the interactions between NRIP and ACTN1 or ACTN2 were calcium-enhanced (lane 5 and 7). As shown in Figure 5D (lane 2), NRIP was found to interact with ACTN2 *in vitro*. Furthermore, we examined whether NRIP associates with ACTN2 *in vivo* by performing co-immunoprecipitation assay and expression vectors for EGFP-tagged NRIP and ACTN2-V5 were co-transfected into 293T cells. The protein lysates were than collected and immunoprtecipitated with anti-EGFP or anti-V5 antibody, respectively (Figure 6). Figure 6C shows that the interaction between NRIP and ACTN2 also exists in mammalian cells (lane 5 and 8). In conclusion, we proved that NRIP interacts with ACTN2 both *in vitro* and *in vivo*.

3.3 The IQ motif of NRIP interacts with the CaM-like domain of ACTN2.

As described previously, NRIP has a calmodulin binding motif, IQ motif, which binds with calmodulin in a calcium-dependent manner (Chang et al, 2011). The IQ motif has been reported that it can associate with proteins containing EF-hand motif (Bahler & Rhoads, 2002; Barry & Bridge, 1993), such as calmodulin or calmodulin-like

proteins. As reported previously, the protein structure of α-actinin are composed of three domains, actin-binding domain (ABD), multiple spectrin repeats (SR) and calmodulin (CaM)-like domain (Sjoblom et al, 2008). Particularly, the carboxyl-terminal domain, calmodulin-like domain is composed of four EF-hand motifs. Therefore, we proposed that NRIP might interact with the CaM-like domain of ACTN2 through its IQ motif. To demonstrate that, we generated the CaM-like domain-truncated construct, GST-ACTN2ΔEF-hand and the IQ motif-deleted construct (NRIPΔIQ), to perform the *in vitro* binding assay (Figure 7 A and C). Firstly, GST-ACTN2 protein and GST-ACTN2ΔEF-hand protein purified separately from bacteria were incubated with His-MBP-NRIP protein and pulled down with GST-conjugated beads. The results show that ACTN2 binds to NRIP mainly through its C-terminal EF-hand motif (Figure 7B, lane 4). Reciprocally, to map which domain of NRIP is responsible for ACTN2 binding, the GST-ACTN2 protein expressed in bacteria was purified and incubated with various His-tagged NRIP fragments including full-length, N-terminus, C-termunus, and IQ-deleted full-length to perform pull down assays. As described in Figure 7D, the ACTN2-binding activity of NRIPΔIQ was significantly reduced compared to the C-terminal and full-length NRIP, indicating that NRIP interacts with ACTN2 through its C-terminal IQ motif. As the data shown in Figure 7, we defined that NRIP can directly interact with the CaM-like domain of ACTN2 through its IQ motif.

3.4 NRIP is a novel Z-disc protein and co-localized with ACTN2.

After a series of protein-protein interaction assays, we demonstrated that NRIP interacts with α-actinin-2 *in vitro* and *in vivo*, defined their interacting domain. Therefore, it raised a question that NRIP is co-localized with ACTN2 in cardiac tissue. To answer the question, the hearts tissues excised from WT and NRIP$^{-/-}$ mice were fixed and co-stained with antibodies against NRIP, ACTN2, or myomesin to perform immunofluorescence assay (IF). IF with control antibodies such as α-actinin-2 and Myomesin labeling Z-disc and M-band, respectively indicated that both WT and NRIP deficient myocardium are well organized with regular cross-striations (Figure 8A). Furthermore, NRIP was found to co-localize with ACTN2 and flanked by M-band labeled by myomesin. The subcellular distribution of NRIP was also confirmed within cardiomyocytes cultured from WT and NRIP-null mice at 12 weeks (Figure 8B). According to the previous definition, a z-disc protein must conform to these requirements. First, a suspected Z-disc protein must co-localize with a bona fide Z-disc protein, such as ACTN2, in immunofluorescence assay. Second, the Z-disc localization of the suspected protein should be detected by electron microscopy with immunogold labelling or biochemical evidences of direct protein–protein interaction with known Z-disc proteins should be proven (Frank et al, 2006). Following these requirements, we

have demonstrated that NRIP interacts with ACTN2 *in vitro* and *in vivo* and these two proteins co-localize in Z-disc. Hence, we characterized that NRIP is a novel Z-disc protein.

3.5 Loss of NRIP reduces I-band width and widen the Z-disc of sarcomere.

Z-disc protein in the traditional concepts is a passive constituent scaffold of sarcomeric structure. It cross-links with thin filament to stabilize the muscle contraction and transmit the force generated by the myofilaments. Many Z-disc proteins have proved that mutations or defects of these proteins disrupt cardiac cytoarchitectural organization and lead to cardiomyopathy (Arber et al, 1997; Hassel et al, 2009; Knoll et al, 2011). Because NRIP has proved as a Z-disc protein and loss of NRIP leads to cardiac hypertrophy. Therefore, it raised a question whether lack of NRIP disrupts sarcommeric structure. To clarify the question, hearts were excised from adult mice, and fixed for transmission electron microscopy (TEM) analysis (Figure 9). As shown in Figure 9, deficiency of NRIP leads to narrower I-band and loose Z-disc. Because of the shortening of I-band, the boundary of H-zone is not clear in myocardium of $NRIP^{-/-}$ mice. To analyze the widths of sarcomeric structures (Figure 10 and Figure 11), the I-band width of $NRIP^{-/-}$ mice was reduced 57.6% (0.11 microns short) and the Z-disc width was 15.2% widen (10.17 nm wide), but the A-band width was similar with WT.

The results of TEM and statistical analyses from hearts of embryonic day 17.5 (E17.5) and postnatal day 2 (P2) (Figure 12 and Figure 13) are corresponded with the consequence from adult mice. The I-band width was reduced in NRIP$^{-/-}$ mice at age E17.5 and P2. To further confirm the results of ultrastructural analysis, the frozen sections of hearts from WT and NRIP$^{-/-}$ were co-stained with phalloidin (F-actin) and anti-actinin antibody to perform immunofluorescence assay (IF) (Figure 14). As shown in Figure 14, the expression pattern of F-actin was more concentrative in Z-disc than the pattern of WT. This might implies deficiency of NRIP affects the expression pattern of F-actin and leads to narrower I-band. Following with the results above, we concluded that loss of NRIP affects the sarcomeric structure, especially the width of I-band. The narrower width of I-band might affect the contractility of hearts, and finally leads to dilated cardiomyopathy progressively.

3.6 Deficiency of NRIP decreases the amplitude of calcium transient.

According to the previous study, we know that NRIP is a calcium-dependent calmodulin binding protein (Chang et al, 2011). Calmodulin (CaM) has been shown as a regulator of many ion channels, such as L-type Ca^{2+} channel, ryanodine receptor and IP3 receptor or as the Ca^{2+} sensor for signaling pathways in cardiac myocytes (Saucerman & Bers, 2012). Defects in ion channels directly affects calcium transient in cardiomyocytes and impairs

contractility of heart muscles (Marks, 2003). Hence, we interested to know whether loss of NRIP affects calcium transient of cardiomyocytes. Adult cardiomyocytes of WT and $NRIP^{-/-}$ mice were isolated at 12 weeks and measured the calcium transient of contractions (Figure 15). The preliminary result of calcium transient measurement shows that the calcium transient amplitude of $NRIP^{-/-}$ mice is lower comparing with WT (Figure 15A). Further analyzed the ratiomeric calcium concentrations of base, peak and the calcium variation of an action, we found that the peak of calcium transient and the total calcium variation of an action are lower than WT (Figure 15B-D). Besides, the time to relaxation is longer in $NRIP^{-/-}$ than in WT (Figure 15F). According the investigation of calcium transient, we speculated NRIP might involve in regulating the calcium concentration in cardiomyocytes. Deficiency of NRIP decreases the variation of calcium concentration and impairs cardiac function.

Chapter 4

DISCUSSION

In summary, loss of NRIP defects cardiac function and leads to cardiac hypertrophy and fibrosis progressively. NRIP affects cardiac function might through interacting with a cardiac Z-disc protein, ACTN2. The IQ motif of NRIP associates with the CaM-like domain of ACTN2. Besides associates with ACTN2 biochemically, NRIP also co-localizes with ACTN2 in Z-disc histologically. Being a novel Z-disc protein, NRIP affects organizations of sarcomere, which narrows I-band and widens Z-disc. Moreover, as a calcium-dependent calmodulin binding protein, deficiency of NRIP decreases the amplitude of calcium transient. According to these results, we speculated that the effects of sarcomeric structure and calcium concentration impair the contractility of myocardium. To compensate the cardiac function, the hearts of NRIP$^{-/-}$ mice trend to hypertrophic cardiomyopathy progressively.

4.1 Deficiency of NRIP leads to cardiac hypertrophy.

According to our study, we know that deficiency of NRIP causes cardiac hypertrophy. In most forms of cardiac hypertrophy, the expression of embryonic genes is increased, including the genes for natriuretic peptides and fetal contractile proteins (Hunter &

Chien, 1999). In our study, we have found the pathological morphology of hypertrophic hearts in NRIP$^{-/-}$ mice, including the thickened ventricular walls and the enlarged cardiac myocytes. To further confirm the cardiac hypertrophy, we might investigate the gene expression of hypertrophic markers, such as atrial natriuretic factor (*ANF*) and brain natriuretic peptide (*BNP*) (Kim et al, 2008; Vikstrom et al, 1998). Because we have found fibrosis in NRIP$^{-/-}$ mice at elder stages, maybe the gene expression of some fibrosis markers, such as connective tissue growth factor (*Ctgf*), procollagen, type I, α2 (*Col1a2)*, and procollagen, type III, α1 (*Col3a1*), could also be investigated.

4.2 NRIP reduces I-band width through affecting proteins involving in actin filament assembly.

Being a Z-disc protein, the defects of NRIP deletion are not similar with other Z-disc proteins, such as MLP or Nexilin, which deletion of MLP or Nexilin leads to Z-disc disarrangement(Arber et al, 1997; Hassel et al, 2009). Lack of NRIP mainly affects the length of actin filament, no matter in embryonic or in adult stages. Actin filament (F-actin) is organized from the polymerization of actin monomer (Ono, 2010; Taylor et al, 2011). Proteins involved in the process of actin polymerization such as CapZ, tropomodulin-1 (Tmod1) and nebulin have been reported that defects of these proteins

affects the length of actin filaments (Cooper & Schafer, 2000; Gokhin & Fowler, 2011; Hart & Cooper, 1999; Littlefield et al, 2001; Littlefield & Fowler, 1998; Witt et al, 2006). From the study of Witt C. et al, deletion of nebulin lead to reduction of I-band length and ~15% extension of Z-disc, these phenotype are similar with our observations. In the study of Witt C et al, they speculated that the loss of nebulin might affect actin filament stability by decelerating actin nucleation, affecting actin termination. Therefore, lengths of actin filaments are reduced. According to the study of Witt c et al, we speculated that NRIP might affect the expression or localization of proteins involving in actin filament formations. For clarify the speculation, we can investigate the protein expression or expression pattern of these proteins in cardiomyocytes of NRIP$^{-/-}$ mice foremost.

4.3 NRIP disrupts myofibrilar arrangements through decreasing gene expressions of genes involving in actin filament formation.

Many Z-disc proteins have been reported as a mechanical or biochemical sensors, such MLP, zyxin and myopodin (Frank et al, 2006). MLP is a sensor of mechanical stimuli, cyclic stretch triggers MLP shuttles from Z-disc to nucleus (Boateng et al, 2007), and then induces downstream gene expression, such as MyoD (Frank et al, 2006). Myopodin is a stress sensor of Z-disc, and it shuttles to nucleus corresponding with the

stress of heat shock (Weins et al, 2001). According to our previous studies, we knew that NRIP is a ligand-dependent transcriptional co-activator of androgen receptor in prostate cancer cell lines. (Chen et al, 2008; Tsai et al, 2005). In addition, except seven WD-40 repeats and one IQ motif, NRIP also contains a nuclear localization sequence (NLS) (Tsai et al, 2005). Consistent with the study of Tsai et al, we found that besides localizing in Z-disc, NRIP is also expressed in nuclei of cardiomyocytes at P2 (data not shown) or adult stages. Furthermore, treated neonatal cardiomyocytes with A23187 (a divalent cation ionophore) (Reed & Lardy, 1972) enhanced the nuclear expression of NRIP (Data not shown). As described previously, NRIP interacts with calmodulin in calcium-dependent manner. In myocytes, calmodulin plays as a calcium sensor to regulate calcium-dependent signaling or activities the ion channels (Frank et al, 2006; Ohrtman et al, 2008). In the study of Wyszynski et al, elevation of the cellular calcium concentration triggers calmodulin to compete the interactions between NMDA receptor and α-actinin, and then to release α-actinin from NMDA receptor(Wyszynski et al, 1997). Therefore, we speculated that in cardiomyocytes calmodulin senses the calcium signals and then associated with NRIP. The interactions of each other release NRIP to translocate into nucleus and to regulate the expressions of genes associated with actin filament formations and stabilizations. To clarify our speculations, the microarray data is essential to help us find out the downstream targets of NRIP. In addition, the

translocation of NRIP and the competition between calmodulin and ACTN2 must further confirm.

4.4 NRIP plays a role in regulating calcium homeostasis.

According to the calcium transient measurement of WT and NRIP$^{-/-}$ mice, we found that loss of NRIP decreases the amplitude of calcium transient. But the mechanism of NRIP regulating calcium homeostasis is still unknown. Many ion channel inhibitors or drugs are applied to investigate the calcium storage or the ability of calcium removal of cells. For examples, caffeine is applied to measure the Ca^{2+} content of sarcoplasmic reticulum (SR) and thapsigargin (TG) or cyclopiazonic acid (CPA) are applied as SR/ER Ca^{2+} pump inhibitors (Campbell et al, 1991; Smith & Steele, 1998). Therefore, ion channel inhibitors or drugs could be applied to further investigate which NRIP participate in which state of calcium regulation, calcium influx or removal.

REFERENCE

Arai M, Alpert NR, MacLennan DH, Barton P, Periasamy M (1993) Alterations in sarcoplasmic reticulum gene expression in human heart failure. A possible mechanism for alterations in systolic and diastolic properties of the failing myocardium. ***Circulation research*** **72: 463-469**

Arber S, Hunter JJ, Ross J, Jr., Hongo M, Sansig G, Borg J, Perriard JC, Chien KR, Caroni P (1997) MLP-deficient mice exhibit a disruption of cardiac cytoarchitectural organization, dilated cardiomyopathy, and heart failure. ***Cell*** **88: 393-403**

Bahler M, Rhoads A (2002) Calmodulin signaling via the IQ motif. ***FEBS letters*** **513: 107-113**

Barry WH, Bridge JH (1993) Intracellular calcium homeostasis in cardiac myocytes. ***Circulation*** **87: 1806-1815**

Boateng SY, Belin RJ, Geenen DL, Margulies KB, Martin JL, Hoshijima M, de Tombe PP, Russell B (2007) Cardiac dysfunction and heart failure are associated with abnormalities in the subcellular distribution and amounts of oligomeric muscle LIM protein. ***American journal of physiology Heart and circulatory physiology*** **292: H259-269**

Broderick MJ, Winder SJ (2005) Spectrin, alpha-actinin, and dystrophin. ***Advances in protein chemistry*** **70: 203-246**

Bruce RA (1974) Methods of exercise testing. Step test, bicycle, treadmill, isometrics. ***The American journal of cardiology*** **33: 715-720**

Campbell AM, Kessler PD, Sagara Y, Inesi G, Fambrough DM (1991) Nucleotide sequences of avian cardiac and brain SR/ER Ca(2+)-ATPases and functional comparisons with fast twitch Ca(2+)-ATPase. Calcium affinities and inhibitor effects. ***The Journal of biological chemistry*** **266: 16050-16055**

Chang SW, Tsao YP, Lin CY, Chen SL (2011) NRIP, a novel calmodulin binding

protein, activates calcineurin to dephosphorylate human papillomavirus E2 protein. ***Journal of virology*** **85: 6750-6763**

Chen PH, Tsao YP, Wang CC, Chen SL (2008) Nuclear receptor interaction protein, a coactivator of androgen receptors (AR), is regulated by AR and Sp1 to feed forward and activate its own gene expression through AR protein stability. ***Nucleic acids research*** **36: 51-66**

Chien KR (1999) Stress pathways and heart failure. ***Cell*** **98: 555-558**

Chiu C, Bagnall RD, Ingles J, Yeates L, Kennerson M, Donald JA, Jormakka M, Lind JM, Semsarian C (2010) Mutations in alpha-actinin-2 cause hypertrophic cardiomyopathy: a genome-wide analysis. ***Journal of the American College of Cardiology*** **55: 1127-1135**

Cooper JA, Schafer DA (2000) Control of actin assembly and disassembly at filament ends. ***Current opinion in cell biology*** **12: 97-103**

Cukovic D, Lu GW, Wible B, Steele DF, Fedida D (2001) A discrete amino terminal domain of Kv1.5 and Kv1.4 potassium channels interacts with the spectrin repeats of alpha-actinin-2. ***FEBS letters*** **498: 87-92**

Frank D, Kuhn C, Katus HA, Frey N (2006) The sarcomeric Z-disc: a nodal point in signalling and disease. ***J Mol Med (Berl)*** **84: 446-468**

Frey N, Olson EN (2003) Cardiac hypertrophy: the good, the bad, and the ugly. ***Annual review of physiology*** **65: 45-79**

Gokhin DS, Fowler VM (2011) Tropomodulin capping of actin filaments in striated muscle development and physiology. ***Journal of biomedicine & biotechnology*** **2011: 103069**

Hart MC, Cooper JA (1999) Vertebrate isoforms of actin capping protein beta have distinct functions In vivo. ***The Journal of cell biology*** **147: 1287-1298**

Hasenfuss G (1998) Alterations of calcium-regulatory proteins in heart failure. ***Cardiovascular research*** **37: 279-289**

Hassel D, Dahme T, Erdmann J, Meder B, Huge A, Stoll M, Just S, Hess A, Ehlermann P, Weichenhan D, Grimmler M, Liptau H, Hetzer R, Regitz-Zagrosek V, Fischer C, Nurnberg P, Schunkert H, Katus HA, Rottbauer W (2009) Nexilin mutations destabilize cardiac Z-disks and lead to dilated cardiomyopathy. *Nature medicine* 15: 1281-1288

Heineke J, Molkentin JD (2006) Regulation of cardiac hypertrophy by intracellular signalling pathways. *Nature reviews Molecular cell biology* 7: 589-600

Hemler ME (1999) Dystroglycan versatility. *Cell* 97: 543-546

Hunter JJ, Chien KR (1999) Signaling pathways for cardiac hypertrophy and failure. *The New England journal of medicine* 341: 1276-1283

Kim Y, Phan D, van Rooij E, Wang DZ, McAnally J, Qi X, Richardson JA, Hill JA, Bassel-Duby R, Olson EN (2008) The MEF2D transcription factor mediates stress-dependent cardiac remodeling in mice. *The Journal of clinical investigation* 118: 124-132

Knoll R, Buyandelger B, Lab M (2011) The sarcomeric Z-disc and Z-discopathies. *Journal of biomedicine & biotechnology* 2011: 569628

Littlefield R, Almenar-Queralt A, Fowler VM (2001) Actin dynamics at pointed ends regulates thin filament length in striated muscle. *Nature cell biology* 3: 544-551

Littlefield R, Fowler VM (1998) Defining actin filament length in striated muscle: rulers and caps or dynamic stability? *Annual review of cell and developmental biology* 14: 487-525

Marks AR (2003) Calcium and the heart: a question of life and death. *The Journal of clinical investigation* 111: 597-600

Mohapatra B, Jimenez S, Lin JH, Bowles KR, Coveler KJ, Marx JG, Chrisco MA, Murphy RT, Lurie PR, Schwartz RJ, Elliott PM, Vatta M, McKenna W, Towbin JA, Bowles NE (2003) Mutations in the muscle LIM protein and alpha-actinin-2

genes in dilated cardiomyopathy and endocardial fibroelastosis. ***Molecular genetics and metabolism*** **80: 207-215**

Ohrtman J, Ritter B, Polster A, Beam KG, Papadopoulos S (2008) Sequence differences in the IQ motifs of CaV1.1 and CaV1.2 strongly impact calmodulin binding and calcium-dependent inactivation. ***The Journal of biological chemistry*** **283: 29301-29311**

Ono S (2010) Dynamic regulation of sarcomeric actin filaments in striated muscle. ***Cytoskeleton (Hoboken)*** **67: 677-692**

Pieske B, Maier LS, Bers DM, Hasenfuss G (1999) Ca2+ handling and sarcoplasmic reticulum Ca2+ content in isolated failing and nonfailing human myocardium. ***Circulation research*** **85: 38-46**

Reed PW, Lardy HA (1972) A23187: a divalent cation ionophore. ***The Journal of biological chemistry*** **247: 6970-6977**

Richardson P, McKenna W, Bristow M, Maisch B, Mautner B, O'Connell J, Olsen E, Thiene G, Goodwin J, Gyarfas I, Martin I, Nordet P (1996) Report of the 1995 World Health Organization/International Society and Federation of Cardiology Task Force on the Definition and Classification of cardiomyopathies. ***Circulation*** **93: 841-842**

Sadeghi A, Doyle AD, Johnson BD (2002) Regulation of the cardiac L-type Ca2+ channel by the actin-binding proteins alpha-actinin and dystrophin. ***American journal of physiology Cell physiology*** **282: C1502-1511**

Sandow A (1952) Excitation-contraction coupling in muscular response. ***The Yale journal of biology and medicine*** **25: 176-201**

Saucerman JJ, Bers DM (2012) Calmodulin binding proteins provide domains of local Ca2+ signaling in cardiac myocytes. ***Journal of molecular and cellular cardiology*** **52: 312-316**

Sjoblom B, Salmazo A, Djinovic-Carugo K (2008) Alpha-actinin structure and regulation. ***Cellular and molecular life sciences : CMLS*** **65: 2688-2701**

Smith GL, Steele DS (1998) Measurement of SR Ca2+ content in the presence of caffeine in permeabilised rat cardiac trabeculae. *Pflugers Archiv : European journal of physiology* 437: 139-148

Taylor MP, Koyuncu OO, Enquist LW (2011) Subversion of the actin cytoskeleton during viral infection. *Nature reviews Microbiology* 9: 427-439

Tsai TC, Lee YL, Hsiao WC, Tsao YP, Chen SL (2005) NRIP, a novel nuclear receptor interaction protein, enhances the transcriptional activity of nuclear receptors. *The Journal of biological chemistry* 280: 20000-20009

Vikstrom KL, Bohlmeyer T, Factor SM, Leinwand LA (1998) Hypertrophy, pathology, and molecular markers of cardiac pathogenesis. *Circulation research* 82: 773-778

Weins A, Schwarz K, Faul C, Barisoni L, Linke WA, Mundel P (2001) Differentiation- and stress-dependent nuclear cytoplasmic redistribution of myopodin, a novel actin-bundling protein. *The Journal of cell biology* 155: 393-404

Witt CC, Burkart C, Labeit D, McNabb M, Wu Y, Granzier H, Labeit S (2006) Nebulin regulates thin filament length, contractility, and Z-disk structure in vivo. *The EMBO journal* 25: 3843-3855

Wyszynski M, Lin J, Rao A, Nigh E, Beggs AH, Craig AM, Sheng M (1997) Competitive binding of alpha-actinin and calmodulin to the NMDA receptor. *Nature* 385: 439-442

Zhang Y, Ye J, Chen D, Zhao X, Xiao X, Tai S, Yang W, Zhu D (2006) Differential expression profiling between the relative normal and dystrophic muscle tissues from the same LGMD patient. *Journal of translational medicine* 4: 53

FIGURES

Table.1 Echocardiographic analysis of $NRIP^{+/+}$ and $NRIP^{-/-}$ mice

Parameters	8 -20 wk		20-30wk		30-40 wk	
	$NRIP^{+/+}$	$NRIP^{-/-}$	$NRIP^{+/+}$	$NRIP^{-/-}$	$NRIP^{+/+}$	$NRIP^{-/-}$
FS,%	39.89±4.09	32.41±18.34	33.06±1.78	22.96±10.37	33.53±5.09	27.37±6.07
EF,%	71.15±4.73	58.47±26.19	62.42±2.81	45.35±17.36	63.04±6.85	53.3±9.66
LVEDD,mm	3.73±0.28	4.52±0.12	3.67±0.58	4.64±0.1	3.52±0.24	4.26±0.24*
LVEDS,mm	2.24±0.19	3.06±0.92	2.51±0.43	3.57±0.4*	2.34±0.28	3.09±0.43
IVSd,mm	0.97±0.34	1.15±0.27	0.59±0.11	0.85±0.049*	0.57±0.04	0.78±0.09*
IVSs,mm	0.69±0.24	0.69±0.11	0.43±0.04	0.66±0.028**	0.47±0.05	0.66±0.12*
LVPWd,mm	1.04±0.17	1.015±0.31	0.64±0.04	0.78±0.049*	0.63±0.04	0.97±0.02**
LVPWs,mm	0.72±0.12	0.63±0.03	0.49±0.08	0.645±0.049	0.51±0.06	0.745±0.049*
HR	381.5±77.25	284.5±0.26	417±47.14	365±65.05	511±37.64	399±8.48*
LVM,mg	146.7±44.88	74.04±0.19	73.25±20.91	155.36±6.32**	65.79±13.78	147.65±28.11**

Table 1. Echocardiographic analysis of *NRIP* mutant (KO) mice.

The cardiac function of wild-type and $NRIP^{-/-}$ mice were analyzed by echocardiography from ages of 8-week to 39-week. Multiple indexes including LVEDD, IVSd, IVSs, IVSs and LVPWd reveal that deficiency of NRIP progressively lead to cardiac hypertrophy. Besides, the measurements of EF and FS imply the cardiac functions of $NRIP^{-/-}$ mice are defected. B6-129 $NRIP^{+/+}$ (n=4), $NRIP^{-/-}$ (n=2), LV, left ventricle; FS, fractional shortening of LV; EF, ejection fraction of LV; EDD, end-diastolic dimension; PW, posterior wall thickness of LV; ESD, end-systolic

dimension. *P <0.05; **P <0.01 represent significant differences between the measurements in $NRIP^{-/-}$ mice compared with $NRIP^{+/+}$ at the same age.

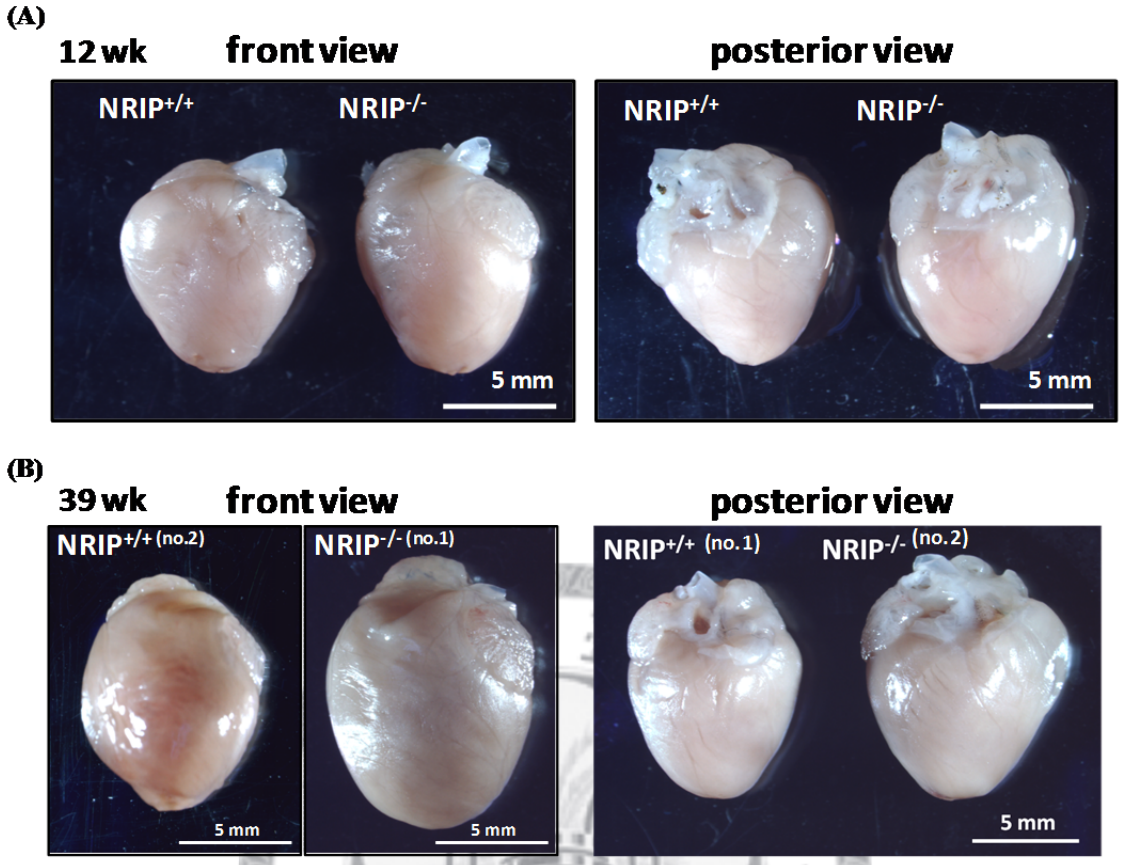

Figure 1. Progressively hypertrophic response of the heart in NRIP-deficient mice.

Hearts from NRIP$^{+/+}$ and NRIP$^{-/-}$ mice at age 12 (A) and 39 (B) weeks were excised, respectively following perfused with 0.5% lidocaine and fixed with 4% paraformaldehyde (PFA) at 4℃ overnight. The hearts of NRIP$^{-/-}$ mice are enlarged and the enlargements are more significant with aging. Scale bar, 5 mm.

(A)

12 wk

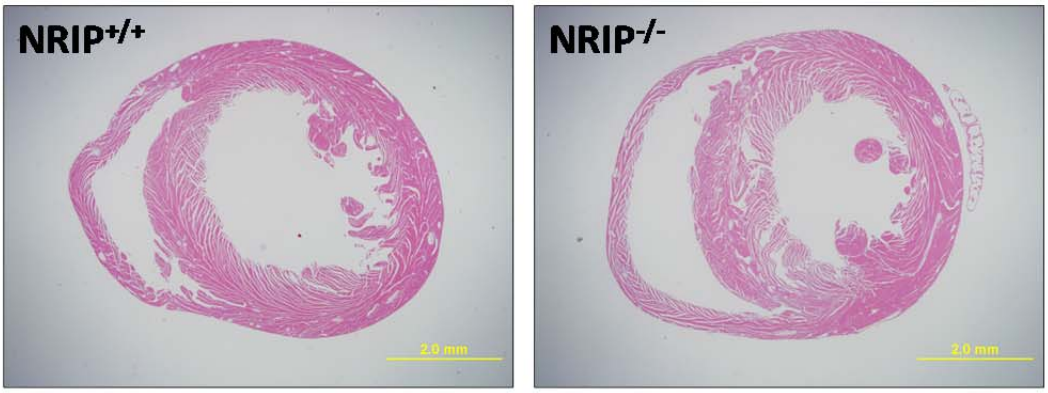

(B)

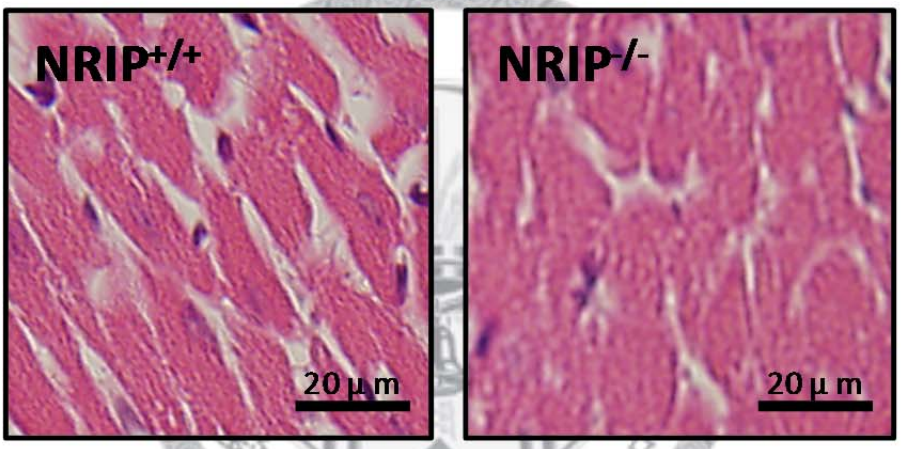

(C)

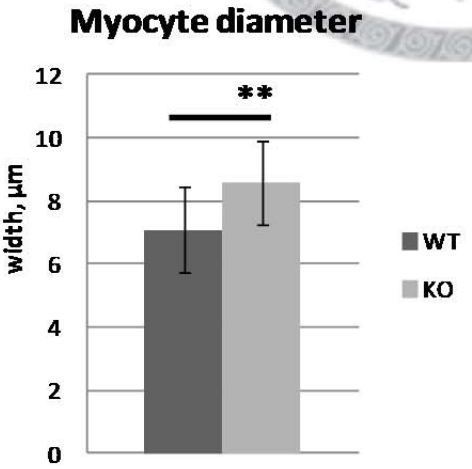

WT	7.1±1.35
KO	8.56±1.35

(D)

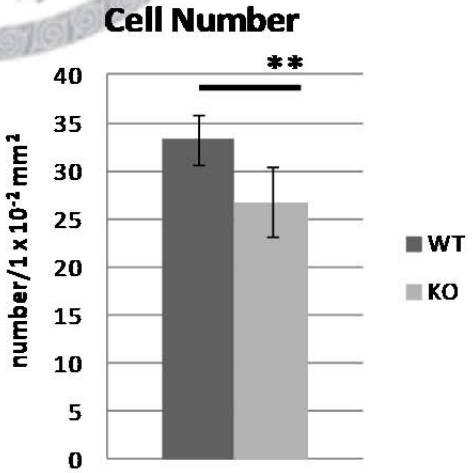

WT	33.25±2.5
KO	26.78±3.67

Figure 2. NRIP deficiency leads to pathological hypertrophy.

Hearts from WT and NRIP-null mice were excised and stained with hematoxylin and eosin (H&E) at age 12 weeks (A). Compared with $NRIP^{+/+}$, the left ventricle walls of $NRIP^{-/-}$ are thicken, including left ventricle posterior wall (LVPW) and interventricular septum (IVS), and the left ventricle dimension is decreased. (B) The myocytes diameters of $NRIP^{-/-}$ mice are widened. (C) The cell width of $NRIP^{-/-}$ cardiomyocyte is enlarged. The short axis was measured as the width of cell by using Image J software. $NRIP^{+/+}$ (n=1, 178 cells), $NRIP^{-/-}$ (n=1, 135 cells). (D) The number of cells per field is reduced in $NRIP^{-/-}$. $NRIP^{+/+}$ (n=1, 4 fields), $NRIP^{-/-}$ (n=1, 9 fields). Results are mean ±SD. **P ＜0.01 versus $NRIP^{+/+}$ .Scale bars, 2.0 mm (A), 20 μm (B).

(A)

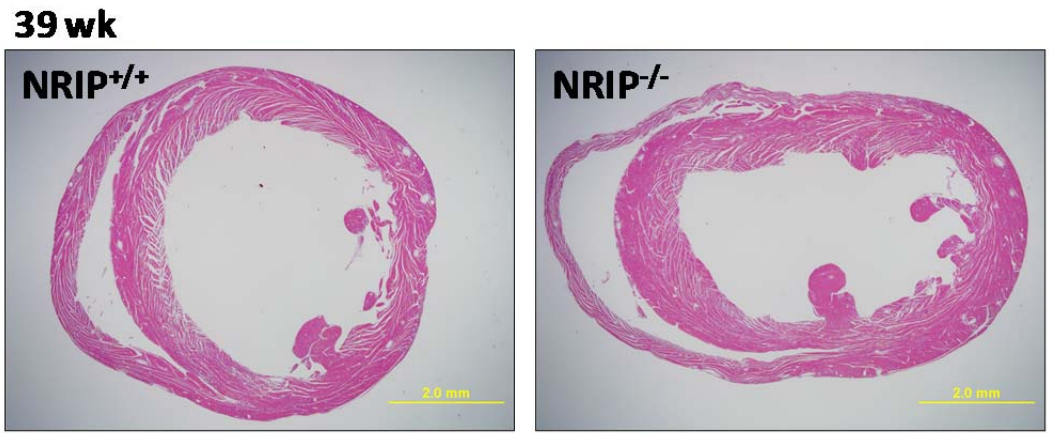

(B)

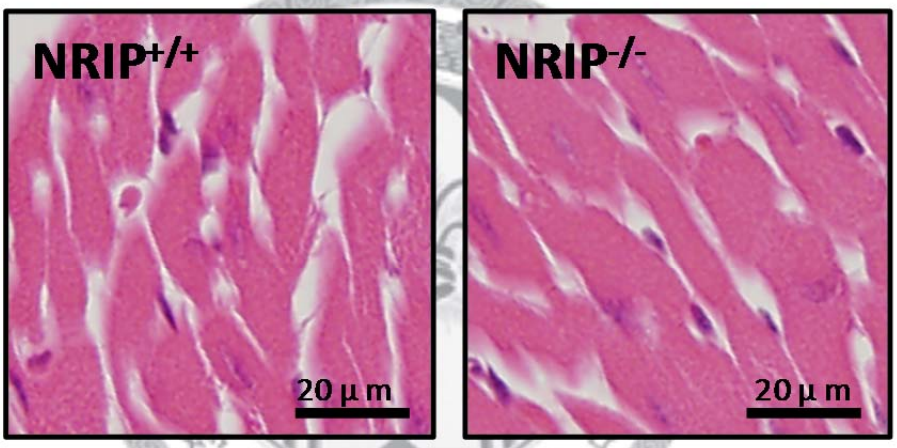

(C)

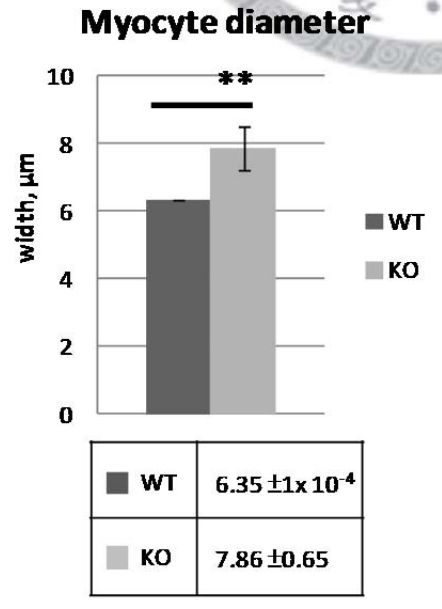

WT	6.35 ±1x 10^{-4}
KO	7.86 ±0.65

(D)

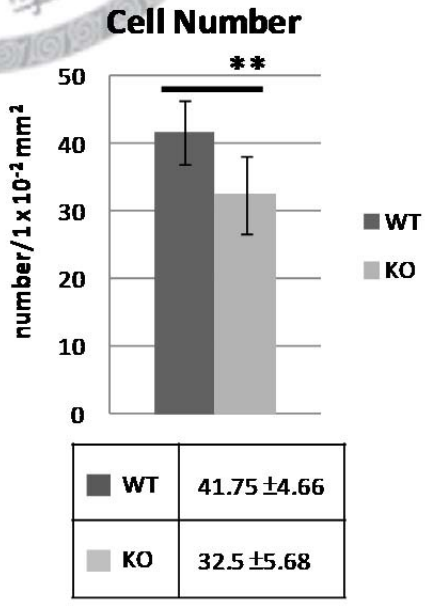

WT	41.75 ±4.66
KO	32.5 ±5.68

Figure 3. Lack of NRIP leads to dilated cardiomyopathy progressively.

Hearts from WT and $NRIP^{-/-}$ mice were excised and stained with hematoxylin and eosin (H&E) at age 39 weeks (A). The LVPW and IVS are thickened and the right ventricle wall is thinned in $NRIP^{-/-}$ mice. The chambers of both left and right ventricles are dilated in hearts of $NRIP^{-/-}$ mice. (B) The cell width of $NRIP^{-/-}$ cardiomyocyte is increased. The quantitative results are shown in panel (C). $NRIP^{+/+}$ (n=2, 182 cells), $NRIP^{-/-}$ (n=2, 200 cells) (D) The number of cells per field is reduced in $NRIP^{-/-}$. $NRIP^{+/+}$ (n=1, 5 fields), $NRIP^{-/-}$ (n=1, 10 fields) Results are mean ±SD. **P ＜0.01 versus $NRIP^{+/+}$ .Scale bars, 2.0 mm (A), 20 μm (B).

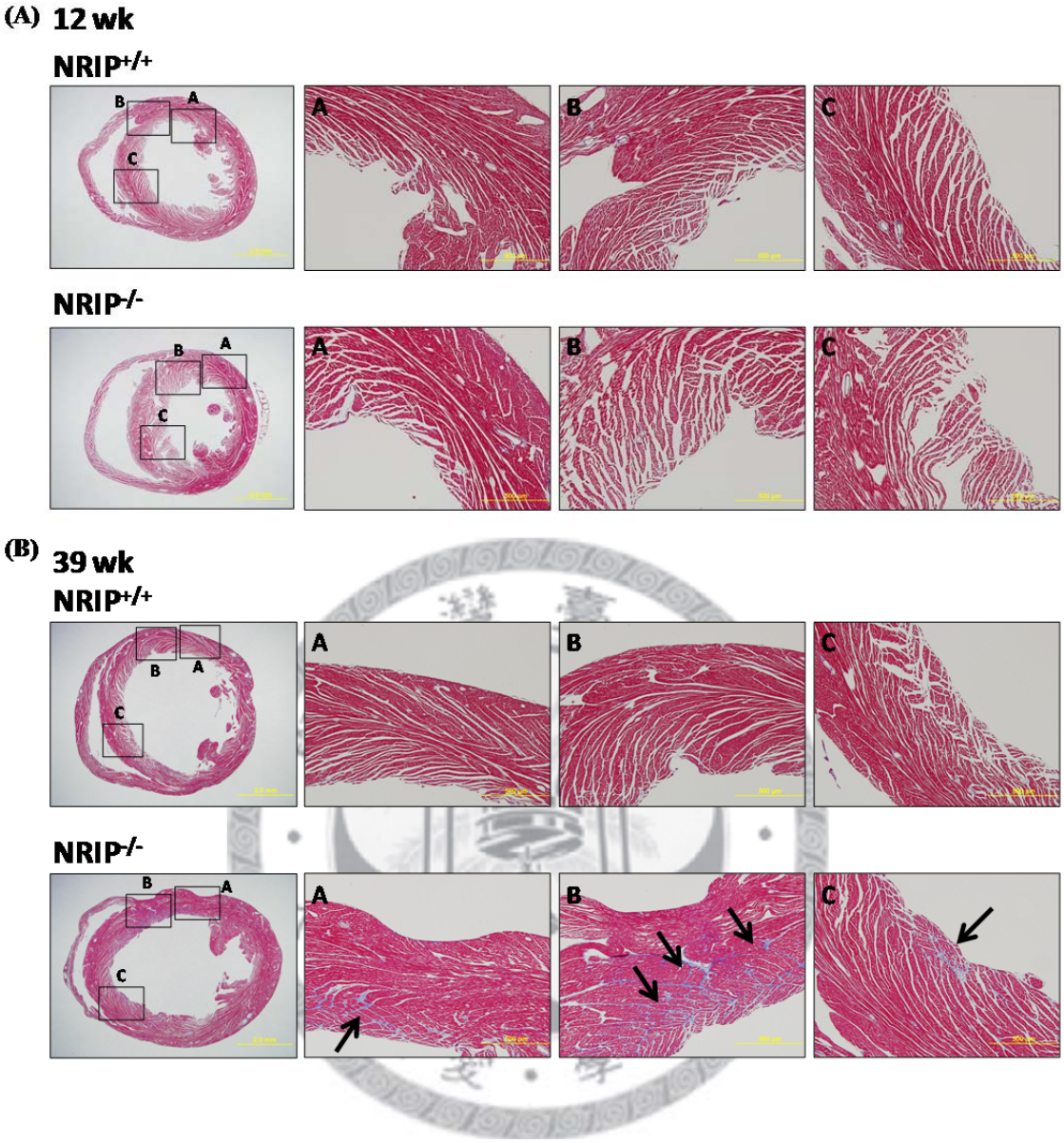

Figure 4. Cardiac fibrosis in LV was observed in NRIP$^{-/-}$ mice at elder stage.

Paraffin-embedded sections from the hearts of WT and NRIP$^{-/-}$ mice were analyzed with Massion's trichrome staining at 12 weeks (A) and 39 weeks (B), respectively. The collagen deposits are shown in blue color. Massive collagen deposits in the left ventricle of NRIP$^{-/-}$ mice at elder stage (B), which are indicated by arroews. Scale bars, 2.0 mm (*Left*); 500 μm (*Right*).

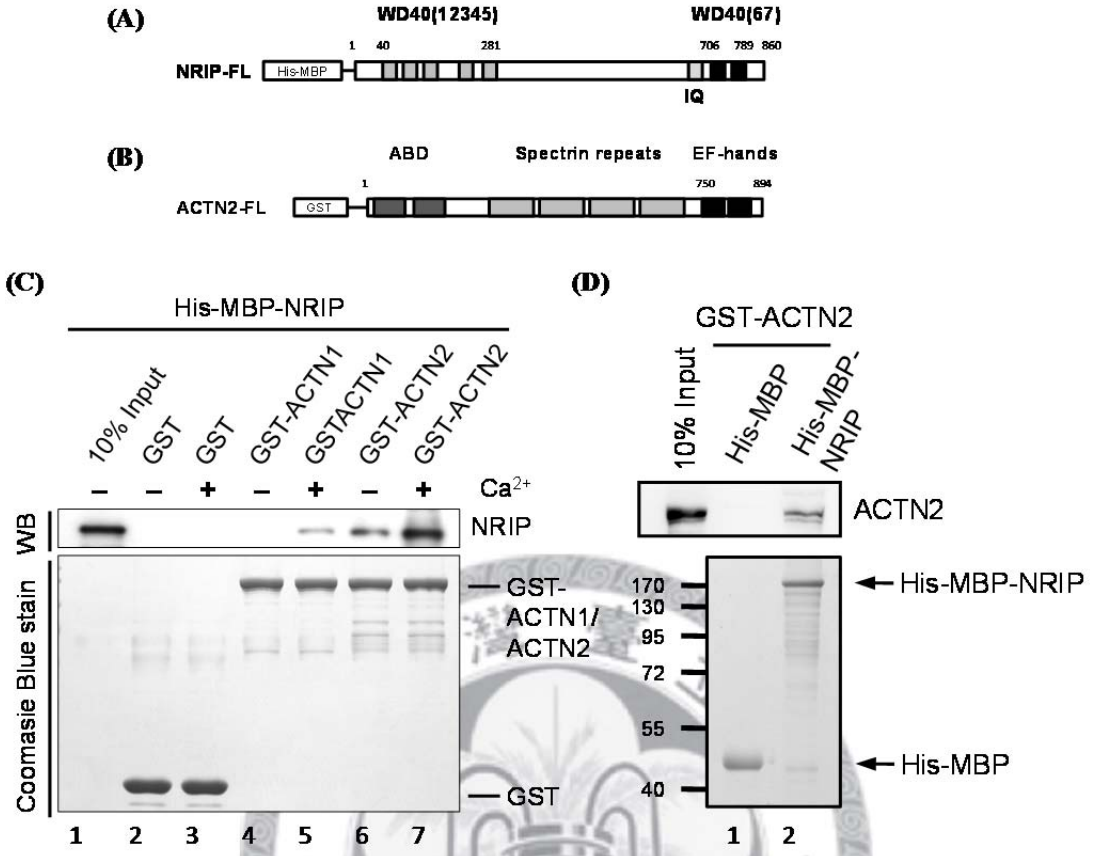

Figure 5. NRIP directly interacts with ACTN2 *in vitro*.

Schematic representations of His-MBP-NRIP (A) and GST-ACTN2 (B) constructs. The protein structure of NRIP contains with seven WD-40 repeats and one IQ motif, which is shown in panel (A). The protein structure of ACTN2 composes of actin-binding domain (ABD), spectrin repeats (SR) and calmodulin-like domain (CaM-like).

(C) Calcium-enhanced interactions between NRIP and α-actinin (1 and 2) via GST pull down assay. The bacterially expressed GST-tagged ACTN1 and ACTN2 proteins were incubated with MBP-NRIP protein in the calcium dependent or independent conditions.

Ten percent of the MBP-NRIP input and the pull-downed lysates were separated by SDS-PAGE, and detected by immunoblotting using anti-NRIP antibody (*Upper*). The purified recombinant proteins were stained with Coomassie blue (*Lower*). (D) Direct interaction between NRIP and ACTN2 via MBP pull-down assay. The bacterially expressed GST-tagged ACTN2 protein was incubated with MBP-NRIP protein. Ten percent of the GST-ACTN2 input and the pull-downed lysates were separated by SDS-PAGE, and detected by immunoblotting using anti-ACTN2 antibody. (*Upper*). The purified recombinant proteins were stained with Coomassie blue (*Lower*).

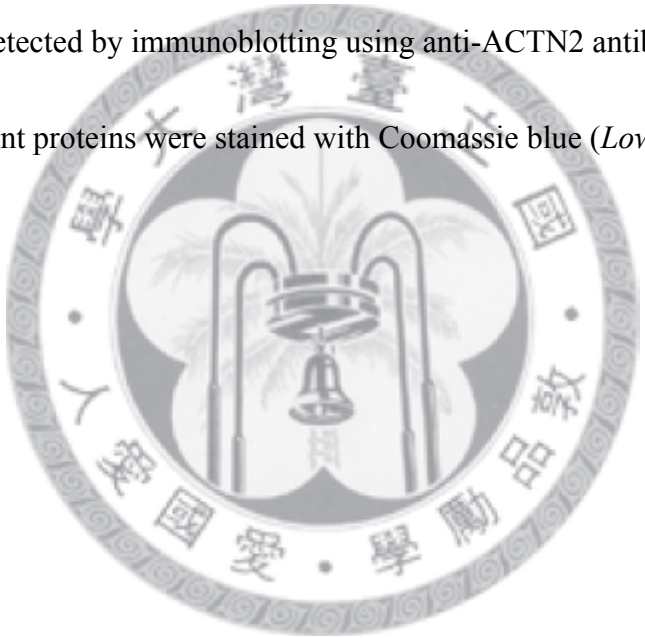

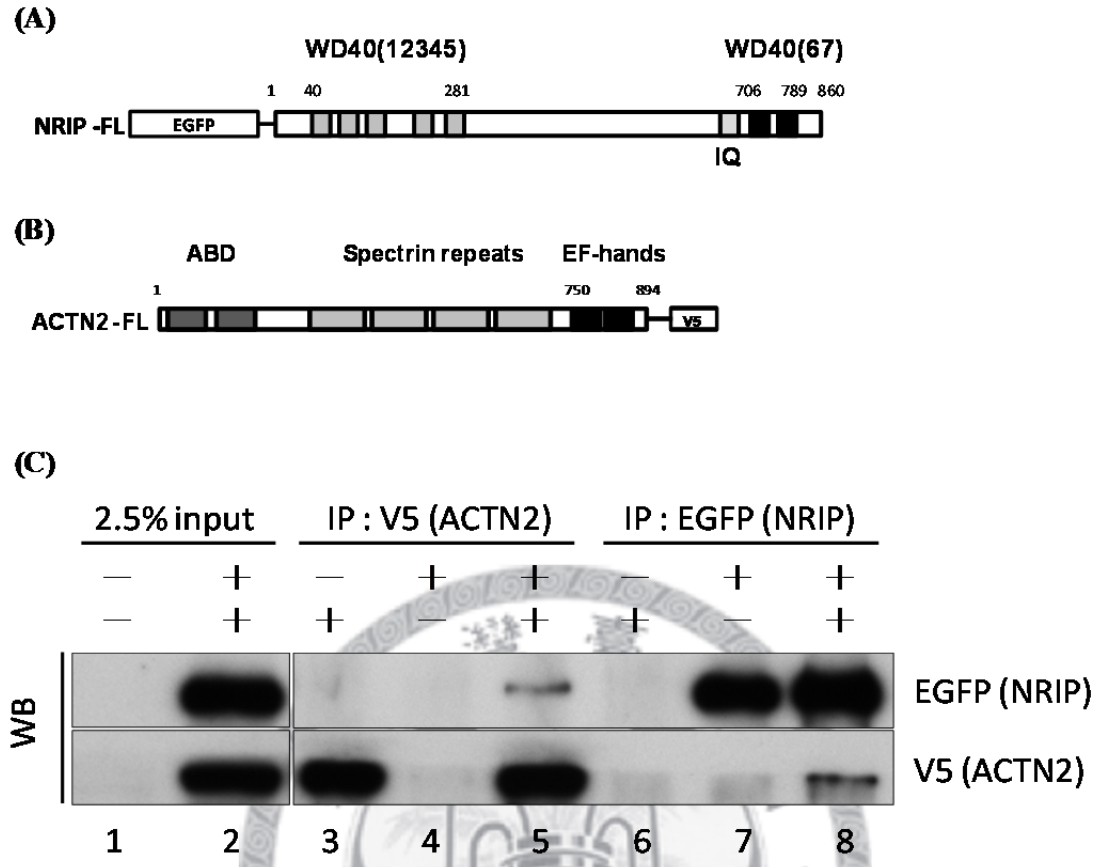

Figure 6. NRIP associates with ACTN2 *in vivo*.

Schematic representations of EGFP-NRIP (A) and ACTN2-V5 (B) constructs. (C) NRIP interacts with ACTN2 *in vivo*. 293T cells were transfected with expression vectors for EGFP tagged NRIP or control vector, along with either V5-tagged ACTN2 expression plasmids or EGFP. Cell extracts were immunoprecipitated with anti-EGFP or anti-V5 antibodies and the immunoprecipitated protein complexes were then separated with SDS-PAGE following immunoblotting was performed with the antibodies indicated.

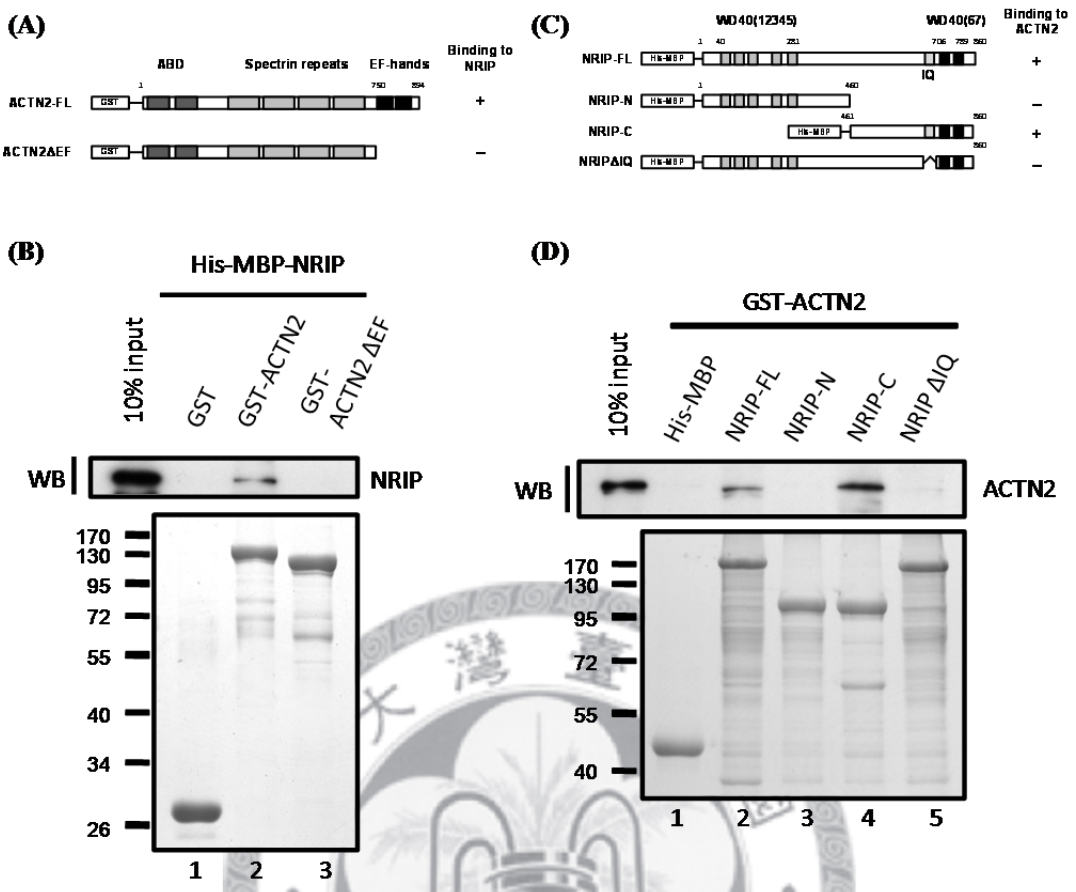

Figure 7. Mapping the interaction domain between NRIP and ACTN2.

(A) Schematic representation of GST-ACTN2 and GST-ACTN2 ΔCaM-like constructs. (B) ACTN2 and ACTN2 truncated EF-hand (ACTN2 1-750) proteins were incubated with His-tagged NRIP, respectively. The results show the EF-hand was responsible for NRIP interaction (lane 3). (C) Schematic representation of His-MBP-NRIP FL, C-termial, N-terminal and ΔIQ constructs. (D) NRIP deletion mapping for the ACTN2 interaction by pull-down assays. GST-tagged ACTN2 proteins were incubated with His-tagged NRIP full-length, C-terminus, N-terminus and ΔIQ, respectively. Without

IQ motif, NRIP can not associate with ACTN2 (lane 3 and 5).As the data shown in (B) and (D), the IQ motif of NRIP can interact with the CaM-like domain of ACTN2.

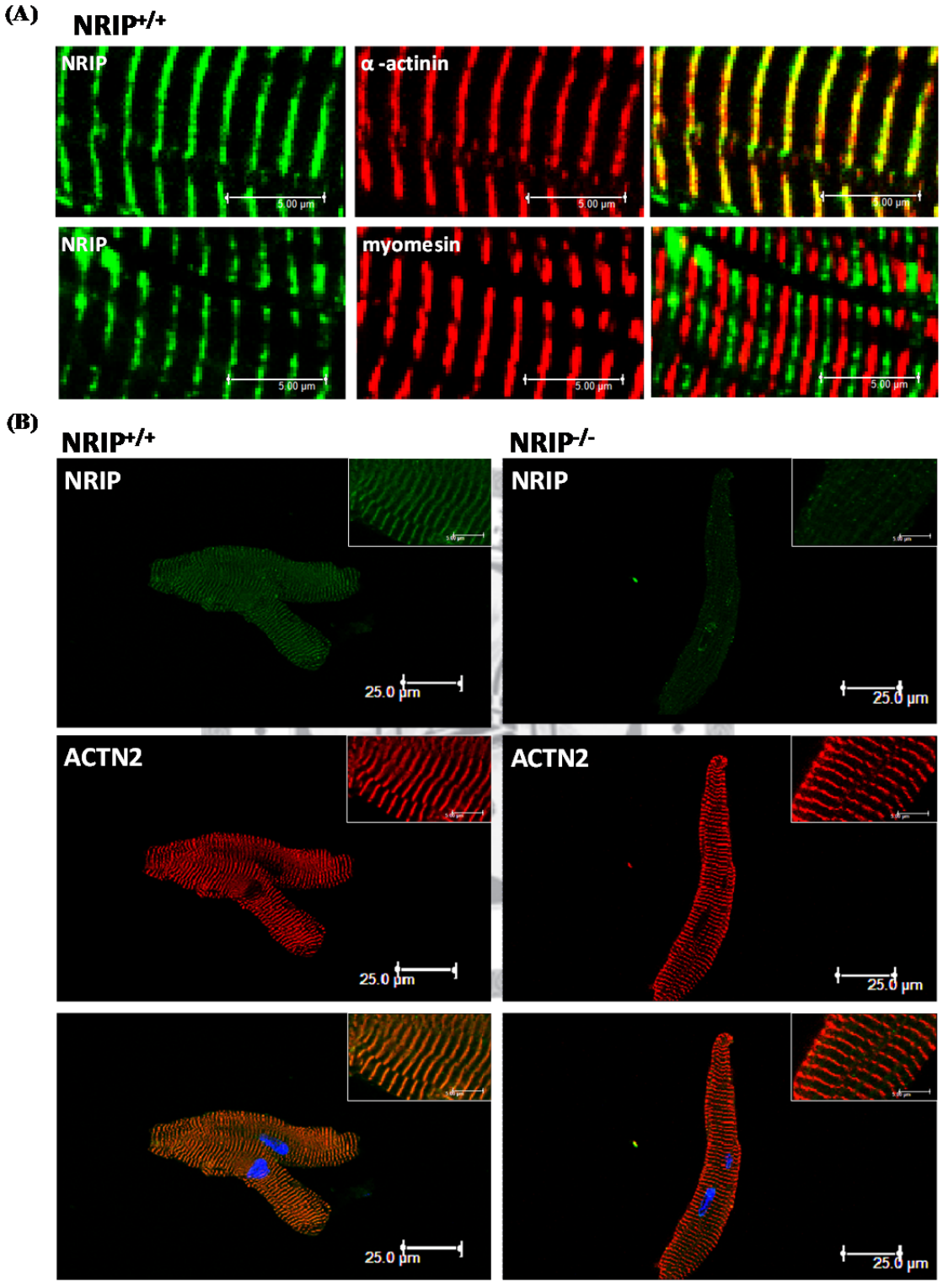
(A)
NRIP+/+
NRIP
α -actinin
NRIP
myomesin
5.00 μm
(B)
NRIP+/+
NRIP-/-
NRIP
ACTN2
25.0 μm

Figure 8. NRIP is a novel Z-disc protein and co-localized with ACTN2.

Structural studies on cardiac myofibrils from WT mice, all fibers were labelled with NRIP (in Green) and in addition with α-actinin or myomesin (in Red) (A), with spatially overlapping epitopes resulting in a yellow color. Myomesin is a representative marker of M-band. The results show NRIP is co-localized with ACTN2 and flanked by myomesin. (B) Cardiomyocytes of WT and NRIP$^{-/-}$ mice were co-stained with NRIP (Green) and α-actinin (Red). NRIP is co-localized with ACTN2 in WT cardiomyocyte. In KO cardiomyocytes, NRIP is not detected and the expression pattern of ACTN2 is not affected. Images were taken by confocal microscopy. Scale bars, 5 μm (A), 25μm (B).

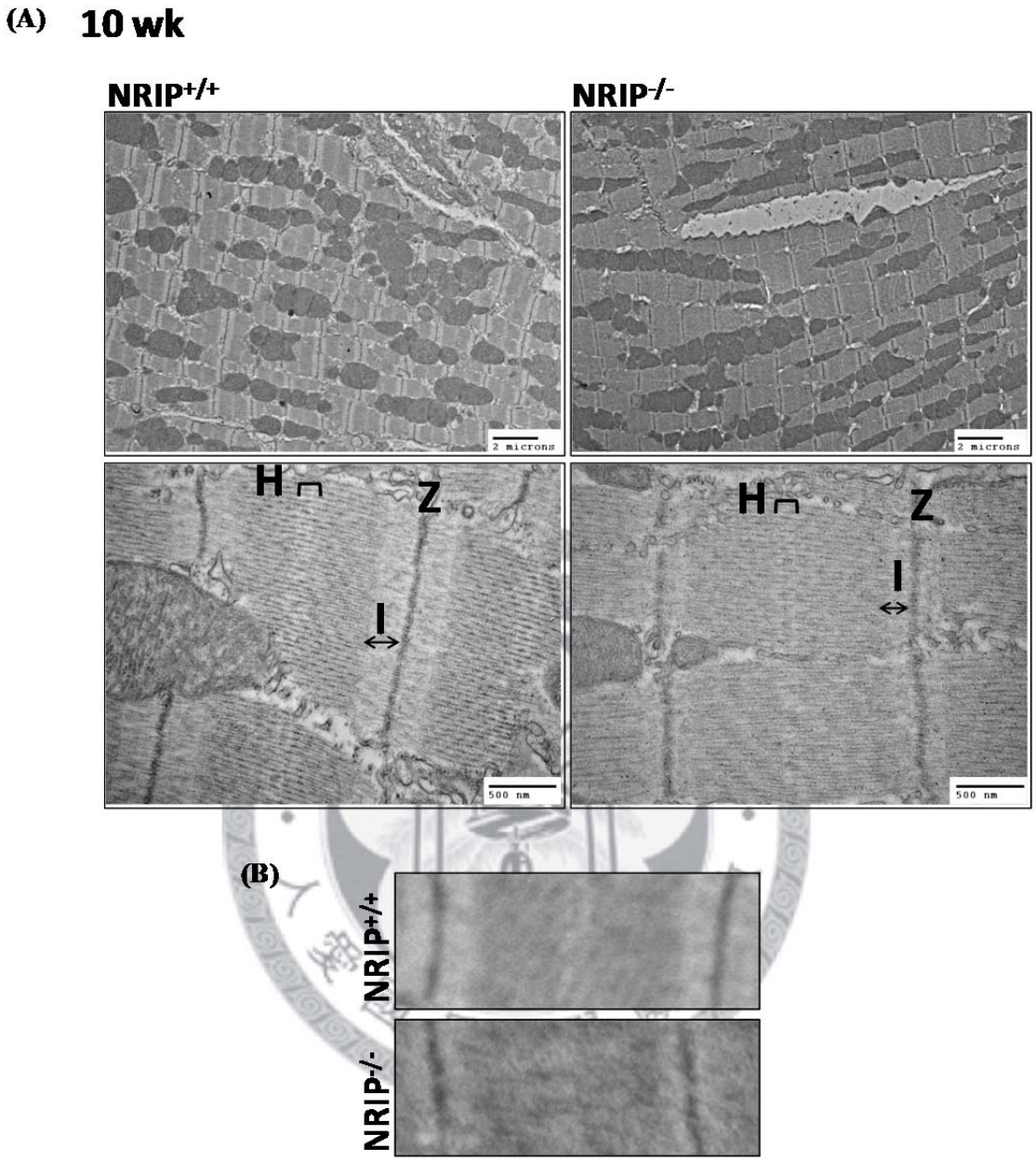

Figure 9. Deficiency of NRIP shows irregular Z-band and narrower I-band in cardiomyocytes via ultrastructural analysis.

The hearts were excised and fixed with 4% paraformaldehyde (PFA) at 4℃ overnight. Parts of LVPW were used to ultrastructural analysis. (A) The sarcomeric structure of WT and NRIP$^{-/-}$ cardiomyocytes was analyzed by transmission electron microscopy

(TEM). Both low (*Upper,* 5000X) and high (*Lower,* 30000X) magnification micrograph shows Z-disc irregularities and I-band shortening in NRIP deficient mice compared with WT. Scale bars, 2 μm (*Upper*); 500 nm (*Lower*) (B) Magnified images of single sarcomere.

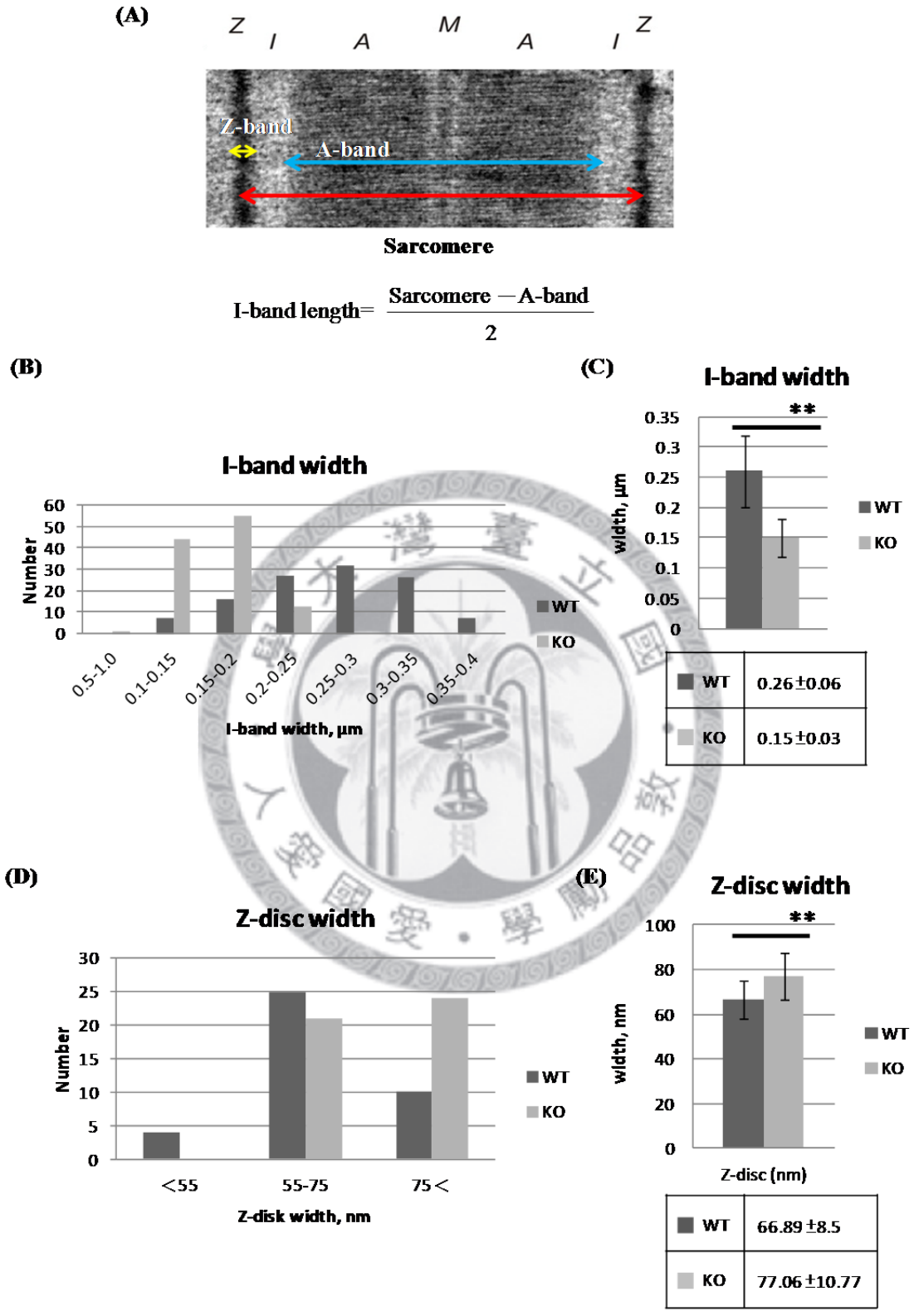

Figure 10. Statistical analysis indicates loss of NRIP narrows down I-band width and affects Z-disc width at age 10 weeks.

(A) Schema depicts the methods of measuring sarcomere, A-band, Z-disc and I-band widths. The distribution of I-band (B) and Z-disc (D) widths. Statistical analysis of I-band (C) and Z-disc (E). The dimensions were measured by Image J software. Data are mean ± SD from 10-week old mice. $NRIP^{+/+}$ (n=2, 115 sarcomeres), $NRIP^{-/-}$ (n=2, 113 sarcomeres) **P < 0.01 versus WT.

(A)

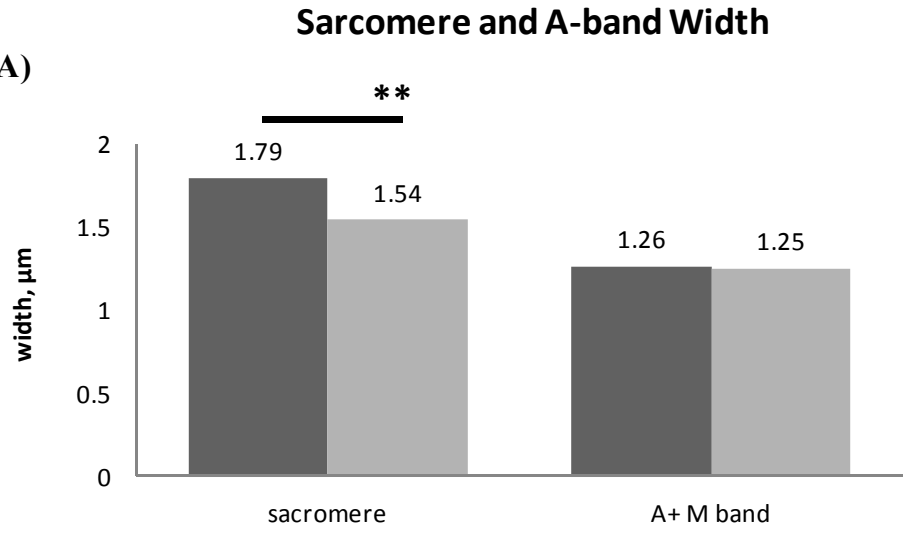

	Sarcomere	A-band
WT	1.79 ±0.16	1.26 ±0.11
KO	1.54 ±0.12	1.25 ±0.09

(B)

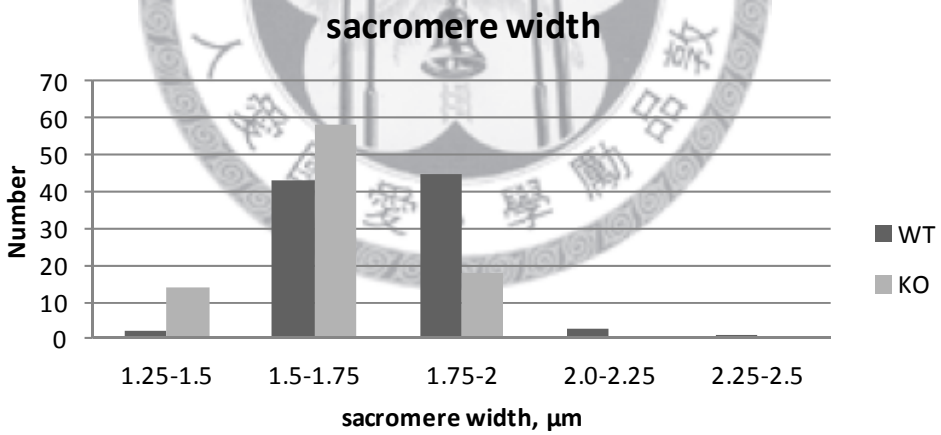

(C)

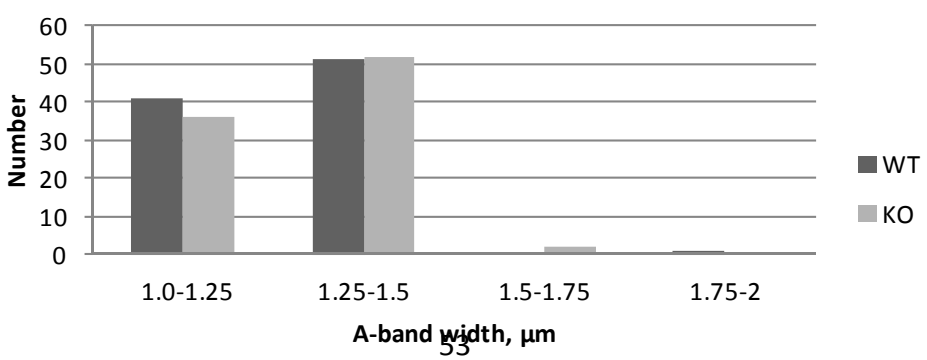

Figure 11. Statistical analysis of sarcomere and A-band widths shows narrower sarcomere width in NRIP$^{-/-}$ myocardium.

(A) Statistical analysis of sarcomere and A-band widths. The sarcomere width is narrower and the A-band width is invariable, compared with WT. Data are mean ± SD from 10-week old mice. **P < 0.01 versus WT. NRIP$^{+/+}$ (n=2, 115 sarcomeres), NRIP$^{-/-}$ (n=2, 113 sarcomeres) (B) The distribution of sarcomere widths. (C) The distribution of A-band widths.

(A) E17.5

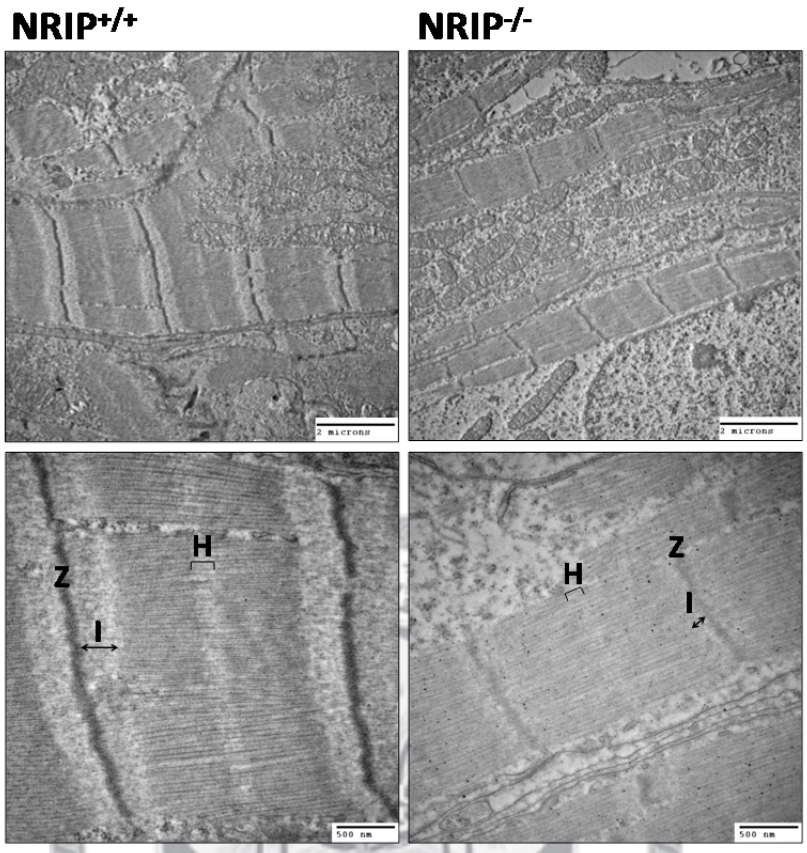
NRIP+/+
NRIP-/-
2 microns
2 microns
H
Z
I
H
Z
I
500 nm
500 nm

(B) P2

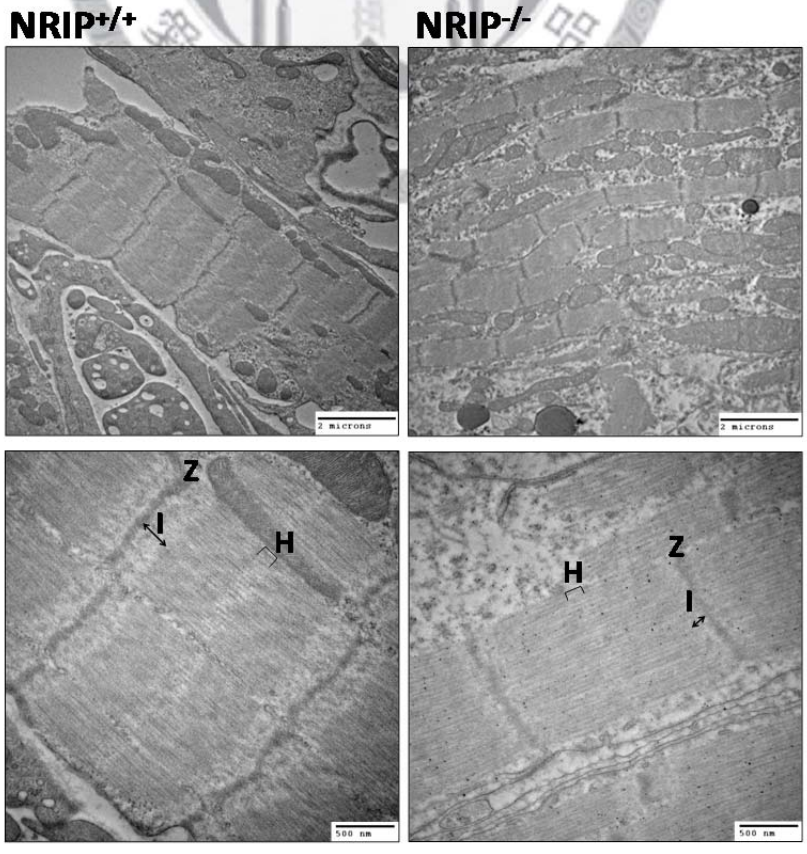
NRIP+/+
NRIP-/-
2 microns
2 microns
Z
I
H
H
Z
I
500 nm
500 nm

Figure 12. Lock of NRIP narrows down I-band width at embryonic and postnatal stages.

Hearts were excised and fixed, and then parts of LVPW were used to ultrastructural analysis. The sarcomeric structure of WT and NRIP$^{-/-}$ cardiomyocytes was analyzed by TEM at age embryonic day 17.5 (E17.5) (A) and postnatal day 2 (P2) (B). Both low (*Upper,* 10000X) and high (*Lower,* 30000X) magnification micrograph shows I-band shortening in NRIP deficient mice compared with WT. Scale bars, 2 μm (*Upper*); 500 nm (*Lower*).

(A)

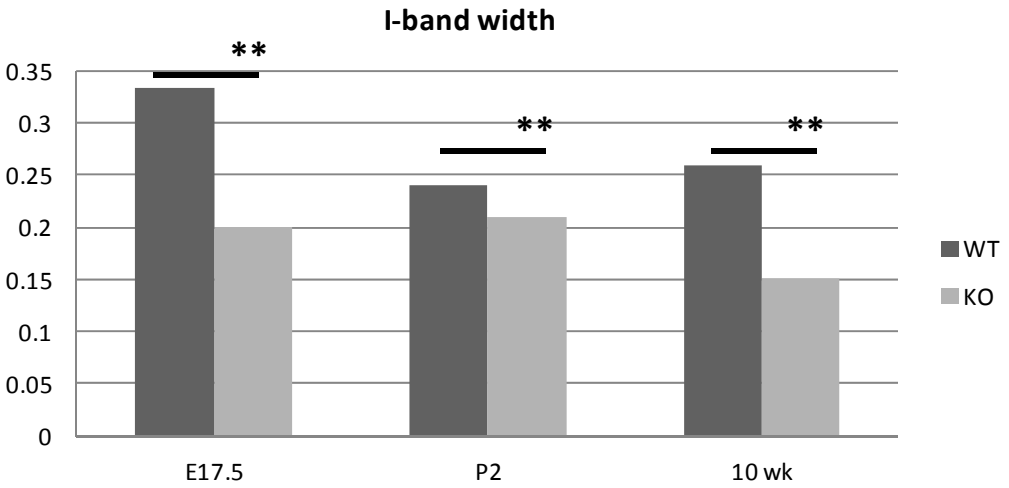

	E17.5	P2	10 wk
WT	0.33 ±0.07	0.24 ±0.08	0.26 ±0.06
KO	0.2 ±0.04	0.21 ±0.04	0.15 ±0.03

(B)

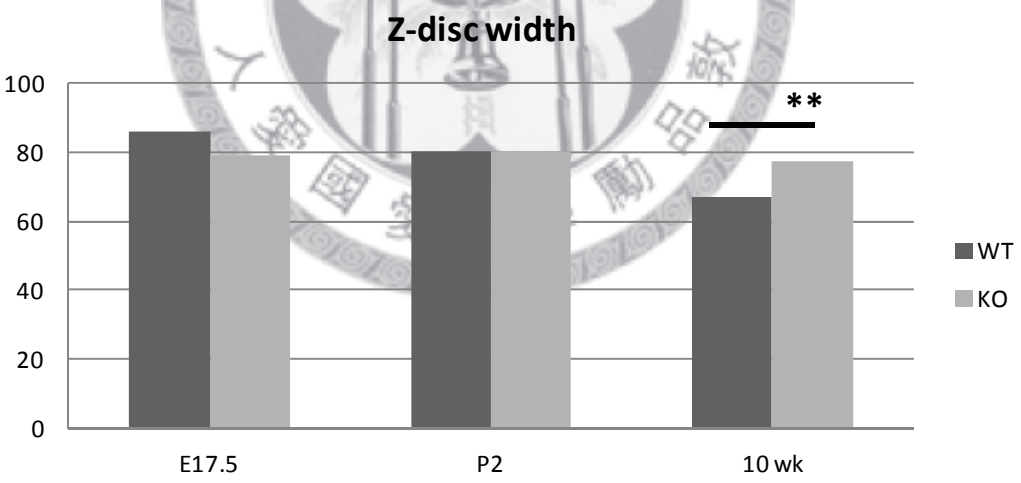

	E17.5	P2	10 wk
WT	85.8 ±16.43	80.27 ±15.66	66.89 ±8.5
KO	78.69 ±19.38	80.28 ±13.25	77.06 ±10.77

Figure 13. The statistical analysis of I-band and Z-disc widths at different stages.

The I-band (A) and Z-disc (B) widths at E17.5, P2 and adult stages. As shown in (A) and (B), deficiency of NRIP narrows I-band width at every stage, but looses Z-disc in adulthood. Data are mean ± SD. **P < 0.01 versus WT. In panel (A), $NRIP^{+/+}$ n=1, 98 sarcomeres (E17.5); 75 sarcomeres (P2), $NRIP^{-/-}$ n=1, n=1, 54 sarcomeres (E17.5); 59 sarcomeres (P2). In panel (B), $NRIP^{+/+}$ n=1, 42 Z-bands (E17.5); 44 Z-bands (P2), $NRIP^{-/-}$ n=1, 46 Z-bands (E17.5 and P2).

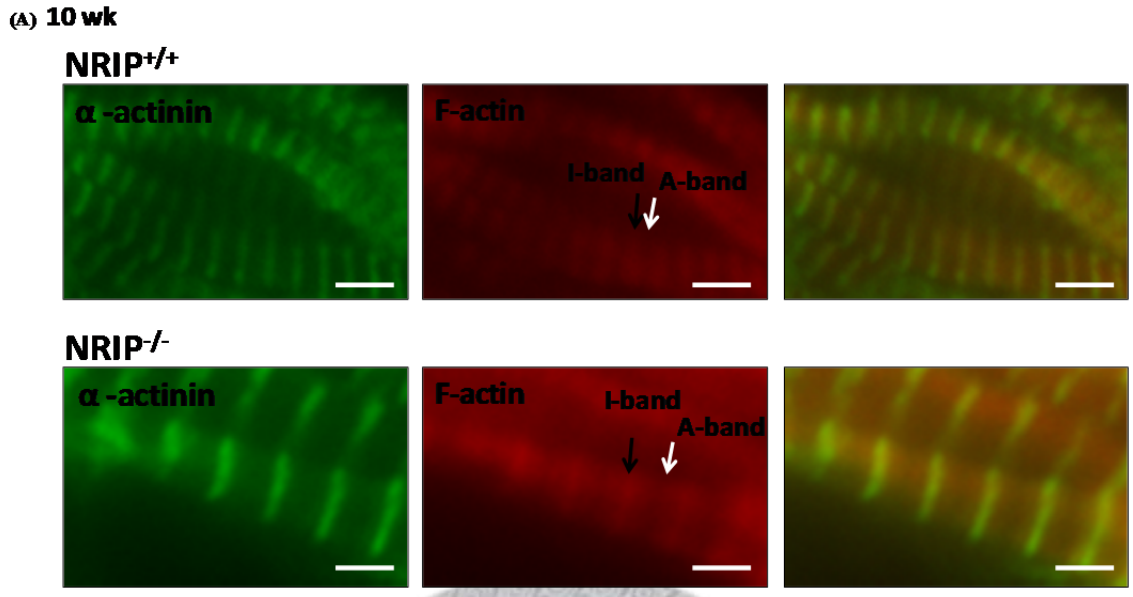

Figure 14. Deficiency of NRIP shows narrower I-band.

(A) Staining of cardiac muscles with phalloidin (F-actin; in Red) and anti-actinin (in Green) antibody. The expression pattern of α-actinin in WT and NRIP$^{-/-}$ is similar, but the pattern of F-actin in NRIP$^{-/-}$ is concentrative in Z-disc comparing with WT. Images were taken by fluorescence microscopy. Scale bar, 2.5 μm.

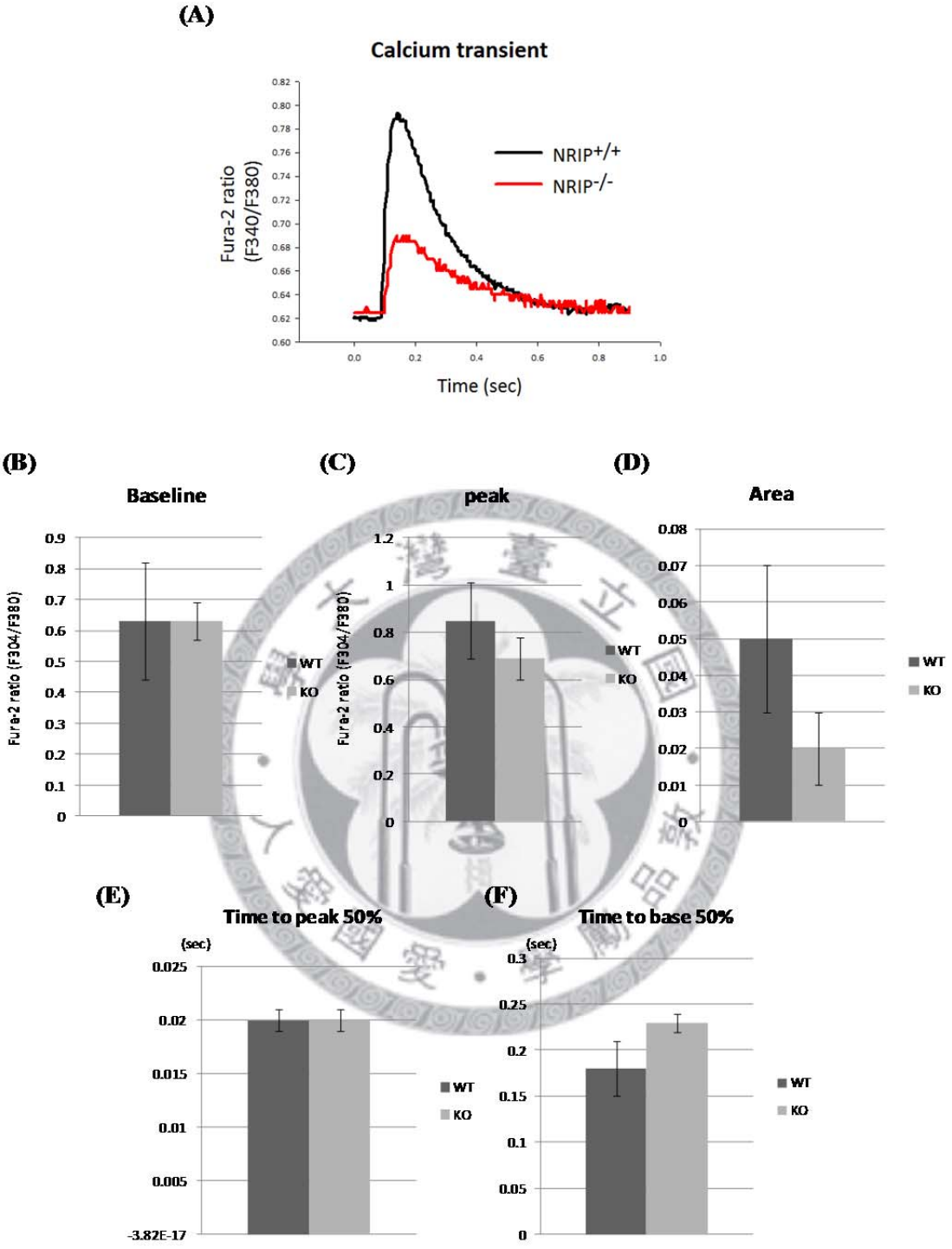

Figure 15. Loss of NRIP decreases calcium transient amplitude and slightly increases the time from peak to baseline.

(A) Ca^{2+} transient illustrations of $NRIP^{+/+}$ and $NRIP^{-/-}$ cardiomyocytes. $NRIP^{+/+}$ (n=2, 6 cells), $NRIP^{-/-}$ (n=1, 2 cells) (B-F) Average data of calcium transient analysis, including baseline, peak, amplitude, time to peak 50% and time to base 50%. $NRIP^{+/+}$ (n=2, 3 cells), $NRIP^{-/-}$ (n=1, 2 cells).Stimulation: 1Hz. Data are mean ± SD. **P < 0.01 versus WT.

APPENDIX

APPENDIX.1

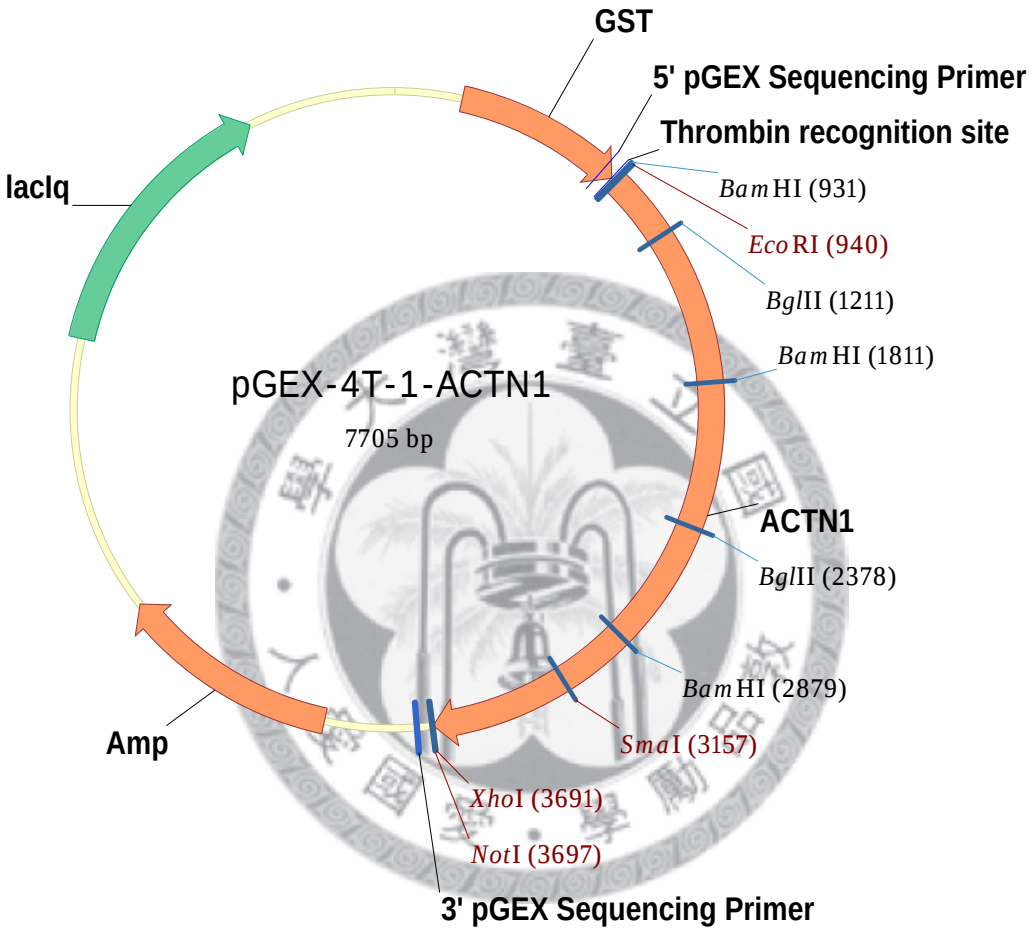

Map1. pGEX-4T-1-ACTN1

APPENDIX.2

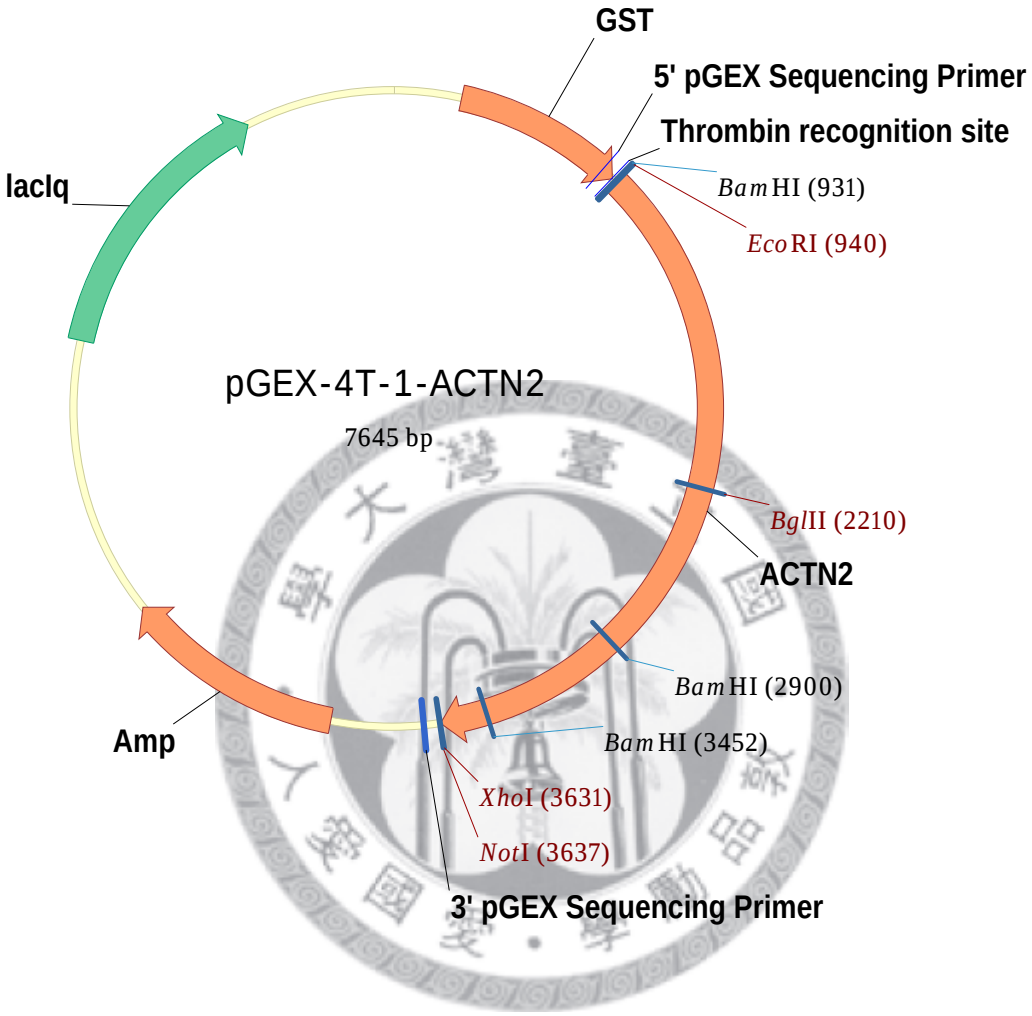

Map2. pGEX-4T-1-ACTN2

APPENDIX.3

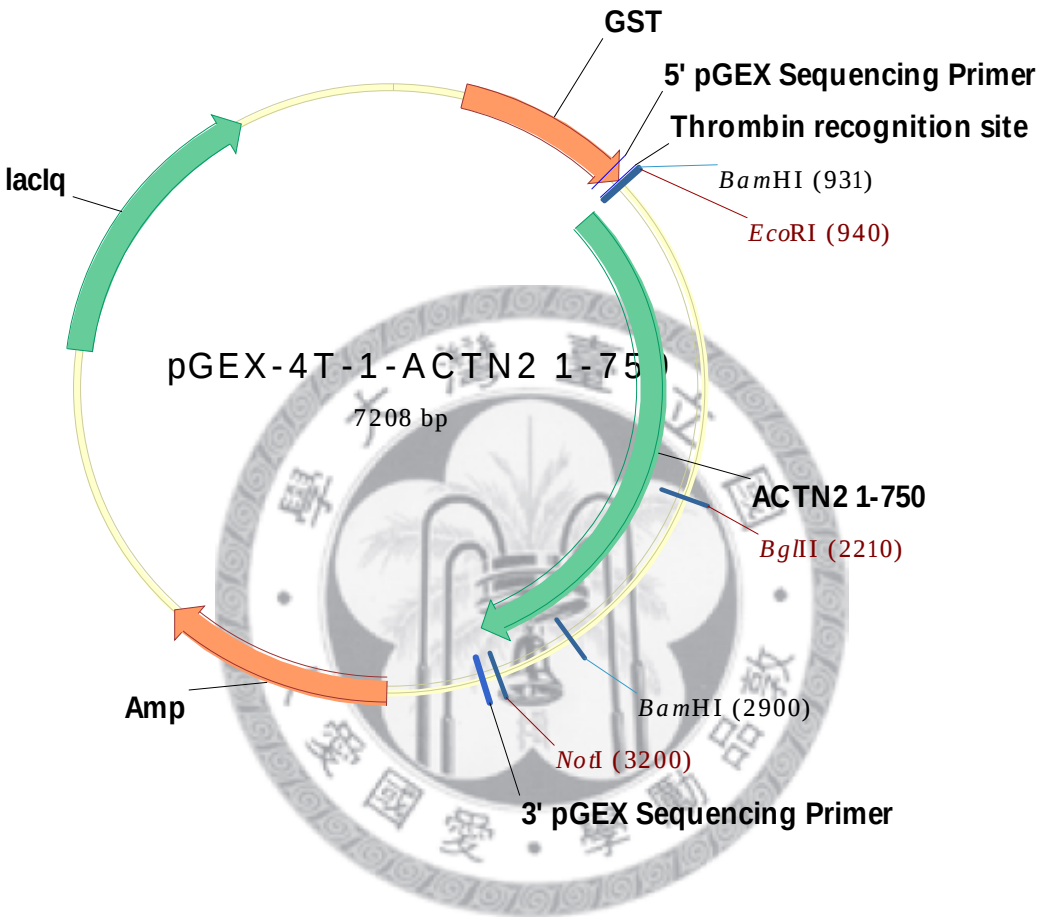

Map3. pGEX-4T-1-ACTN2 1-750.

APPENDIX.4

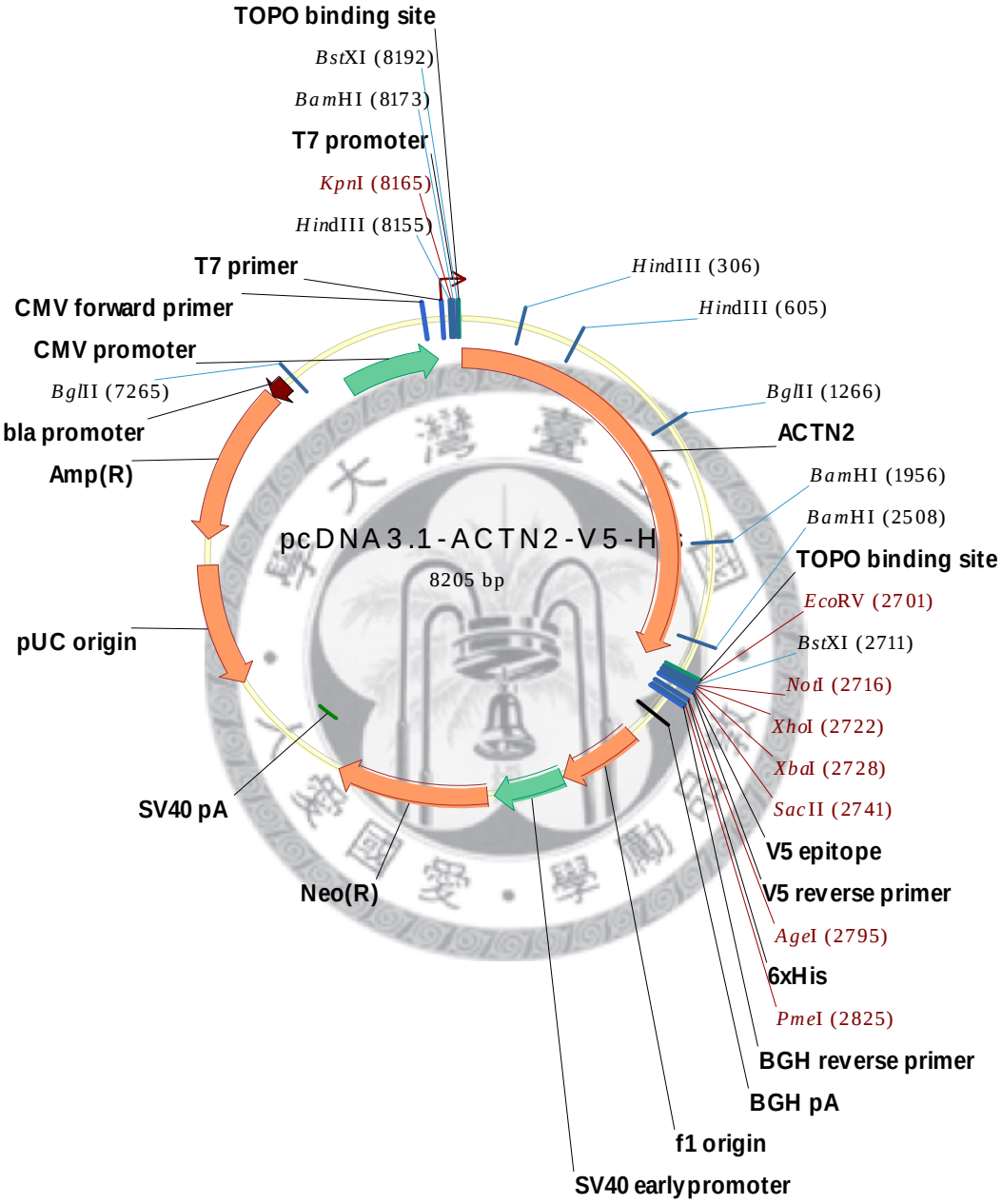

Map 4. pcDNA3.1-ACTN2-V5-His.

APPENDIX.5

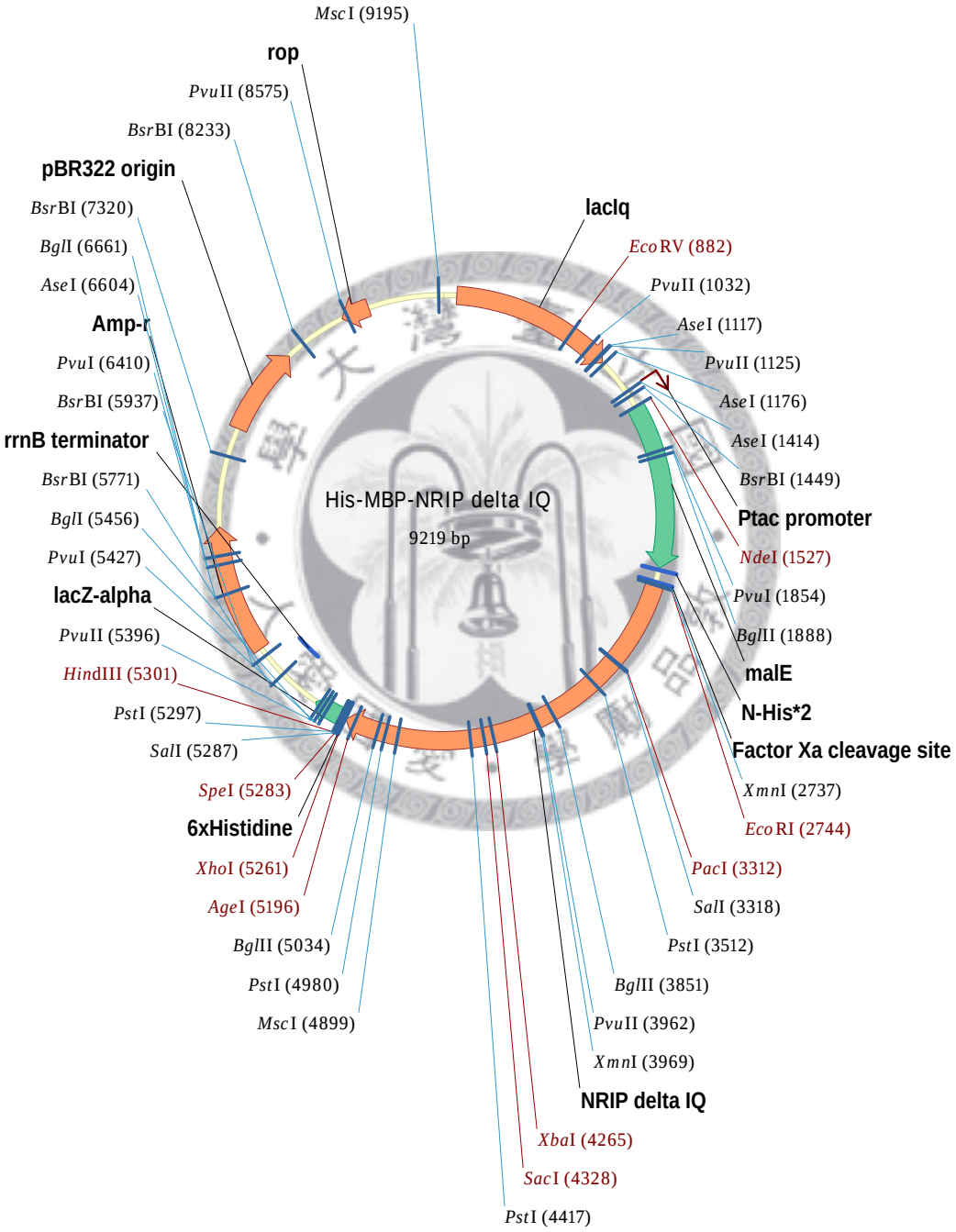

Map 5. His-MBP-NRIP delta IQ